SQSTM1 (PM045; MBL), antiubiquitin (P4D1; Santa Cruz), and anti-LC3 (PD014; MBL). The rabbit polyclonal antibodies directed against mouse Nrf1 that were used in chromatin immunoprecipitation (ChIP) experiments were raised by immunizing rabbits with a purified recombinant six-histidine (6×His)-tagged Nrf1 protein (residues 292 to 741) that was expressed in *Escherichia coli*. The resultant antibodies were subjected to affinity purification.

Plasmids and recombinant proteins. The 3×Flag mouse Nrf1 expression plasmid was described previously (19). Human CK2α (hCK2α) and hCK2β cDNAs were subcloned into pcDNA3 (HA). The ubiquitin-fused luciferase reporter (Ub-FL) reporter plasmid was kindly provided by David Piwnica-Worms (20). The 3xPSMA4-ARE-Luc (Luc stands for luciferase) plasmid was kindly provided by Raymond J. Deshaies (17). The pRBGP2-Luciferase plasmid was described previously (21). The MafK expression plasmid was described previously (22). PCR-amplified Nrf1 fragments were subcloned into pET-15b. Recombinant 6× histidine-tagged Nrf1 fragments were expressed in *E. coli* and purified with nickel-nitrilotriacetic acid (Ni-NTA)–agarose (Qiagen). Recombinant CK2α was described previously (23).

Cell culture and transfection. HeLa cells, COS7 cells, and MCF10A cells were cultured in Dulbecco's modified Eagle's medium (DMEM) (Wako) that was supplemented with 10% fetal calf serum (FCS) (Invitrogen), 4,500 mg/liter glucose, 40 μg/ml streptomycin, and 40 units/ml penicillin. Mouse embryonic fibroblasts (MEFs) were cultured in Iscove's modified Dulbecco's medium (IMDM) (Wako) that was supplemented with 10% FCS, 2 mM glutamine (Invitrogen), 40 μg/ml streptomycin, and 40 units/ml penicillin. The transfection of plasmid DNA and small interfering RNA (siRNA) was achieved using Lipofectamine Plus and Lipofectamine 2000 (Invitrogen), respectively.

siRNA knockdown experiment. The cells were cultured for 24 h in medium without antibiotics. The cells were transfected twice with 40 nM siRNA (at 24 and 48 h after plating) using Lipofectamine 2000. The sequences of the siRNAs employed in the present study are listed in Table S3 in the supplemental material. Twenty-four hours after the last transfection, the cells were utilized for each experiment. For immunoblot analysis, the cells were lysed with an SDS sample buffer (50 mM Tris-HCl [pH 6.8], 10% glycerol, and 1% SDS), and the resultant whole-cell extracts were subjected to immunoblotting with the antibodies indicated in Fig. 1B, 2A and C, 5C, and 6C.

RNA extraction and real-time quantitative PCR. Total RNA was extracted from cells with the RNeasy minikit (Qiagen) and subjected to cDNA synthesis with random hexamer primers and Moloney murine leukemia virus (M-MLV) reverse transcriptase (Invitrogen) according to the manufacturer's instructions. Real-time quantitative PCR was performed with FastStart Universal SYBR (Roche) and ABI Prism 7900 (Life Technologies). The PCR primers employed in the present study are listed in Table S4 in the supplemental material.

Immunoprecipitation and immunoblot analysis. COS7 cells were treated with the proteasome inhibitor MG132 (Peptide Institute) at a concentration of 10 μM for 4 h and subjected to preparation as whole-cell extracts with lysis buffer (50 mM Tris-HCl [pH 8.0], 10% glycerol, 100 mM NaF, 50 mM NaCl, 2 mM EDTA, 2 mM sodium orthovanadate, 10 mM sodium pyrophosphate, 10 mM β-glycerophosphate, 0.1% NP-40, 1 mM phenylmethylsulfonyl fluoride (PMSF), and 1× protease inhibitor cocktail [Roche]). The whole-cell extracts were subjected to immunoprecipitation with anti-Flag M2 affinity gels (Sigma) at 4°C for 2 h. After the anti-Flag M2 affinity gels were washed with wash buffer (50 mM Tris-HCl [pH 7.4], 150 mM NaCl, and 0.1% NP-40) three times, the immunocomplexes were eluted by boiling in SDS sample buffer and subjected to immunoblot analysis using the antibodies indicated in the figures. The blots were treated with a horseradish peroxidase-conjugated secondary antibody (Invitrogen) and were developed with an enhanced chemiluminescence (ECL) kit (GE Healthcare).

Chromatin immunoprecipitation. HeLa cells grown in a 100-mm dish were cross-linked in 1% formaldehyde for 10 min, followed by quenching with 1/10 volume of 1.25 M glycine solution and two washes with phosphate-buffered saline (PBS). The cells were lysed in cell lysis buffer (5 mM Tris-HCl [pH 8.0], 85 mM KCl, 0.5% NP-40, 1 mM PMSF, and 1× protease inhibitor cocktail). Nuclear extracts were prepared by treating the nuclear pellets with ChIP SDS lysis buffer (50 mM Tris-HCl [pH 8.0], 10 mM EDTA, 1% SDS, 1 mM PMSF, and 1× protease inhibitor cocktail), followed by sonication using a Bioruptor (Tosho Electric Co., Ltd.). Proteins were immunoprecipitated in ChIP dilution buffer (16.7 mM Tris-HCl [pH 8.0], 167 mM NaCl, 1.2 mM EDTA, 0.01% SDS, 1.1% Triton X-100, 1 mM PMSF, and 1× protease inhibitor cocktail) using the antibodies indicated in the figures and Dynabeads protein G (Invitrogen). The beads were washed with low-salt wash buffer (20 mM Tris-HCl [pH 8.0], 150 mM NaCl, 2 mM EDTA, 0.1% SDS, and 1% Triton X-100), high-salt wash buffer (20 mM Tris-HCl [pH 8.0], 500 mM NaCl, 2 mM EDTA, 0.1% SDS, and 1% Triton X-100), lithium wash buffer (10 mM Tris-HCl [pH 8.0], 250 mM LiCl, 1% deoxycholate, 1 mM EDTA, and 1% NP-40), and Tris-EDTA (TE) buffer. Cross-linking was reversed overnight at 65°C in ChIP elution buffer (1% SDS and 50 mM $NaHCO_3$). ChIPed DNA was then treated with RNase A and proteinase K, purified with a QIAquick PCR purification kit (Qiagen), and analyzed by real-time quantitative PCR.

Bioluminescence recordings. HeLa cells were transfected with a Ub-FL reporter in combination with the indicated siRNAs or 3× Flag Nrf1 (wild-type or S497A mutant) vectors using Lipofectamine 2000. Forty-eight hours after transfection, the cells were treated with 0.1 mM D-luciferin (Toyobo), and bioluminescence was measured and integrated for 1 min at 10-min intervals with a luminometer (AB-2550 Kronos Dio; Atto). Epoxomicin was added to the culture medium 1 to 2 h after the start of the measurement.

Luciferase reporter assay. Cells expressing the reporters indicated in the legends for Fig. 3A and B, 5A and D to F, and 6 were lysed, and the luciferase activities were measured with the PicaGene luciferase assay system (Toyo Ink) and a Berthold Lumat LB9507 luminometer.

Measurement of proteasome activity. HeLa cells transfected with the siRNAs indicated in the figures were treated with 10 nM epoxomicin for 24 h. The proteasome activity was determined by measuring chymotrypsin activity with Proteasome-Glo chymotrypsin-like cell-based assay (Promega) according to the manufacturer's instructions.

FIG 1 Nrf1 regulates the expression of proteasome subunit genes that are induced by proteasome inhibition in HeLa cells. (A) siRNA-mediated knockdown of Nrf1. HeLa cells transfected with control (Ctrl) siRNA or Nrf1 siRNA were treated with DMSO or 1 μM MG132 for 16 h. mRNA expression levels of Nrf1 were determined by real-time quantitative PCR analysis. The values were normalized to 18S rRNA values and presented as the means plus standard deviations (SD) (error bars) ($n = 3$). (B) MG132 induces the accumulation of Nrf1 proteins. HeLa cell extracts were prepared at the indicated time points after 1 μM MG132 treatment and subjected to immunoblot analysis with anti-Nrf1 (αNrf1) (H-285) antibody. αα-tubulin, anti-α-tubulin antibody. (C) Nrf1-dependent induction of proteasome genes. The mRNA expression levels of the indicated genes were determined by real-time quantitative PCR. The expression level in the cells transfected with the control siRNA and treated with DMSO was set at 1. The values were normalized to 18S rRNA values and presented as the means plus SD ($n = 3$). (D) The heat map shows the mRNA expression levels of the indicated genes that correspond to the graphs in Fig. 1C and data not shown. The values were normalized to 18S rRNA values and presented as the means of at least three replicates. The N/C ratio is the ratio of the expression level in Nrf1 siRNA-treated cells to the expression level in control siRNA-treated cells with MG132 treatment. The color bar indicates the range of the expression ratios in log space. (E) Time course of expression of PSMC4, PSMA4, GSTA4, and NQO1 upon MG132 treatment. The values were normalized to 18S rRNA values and presented as the means ± SD ($n = 5$).

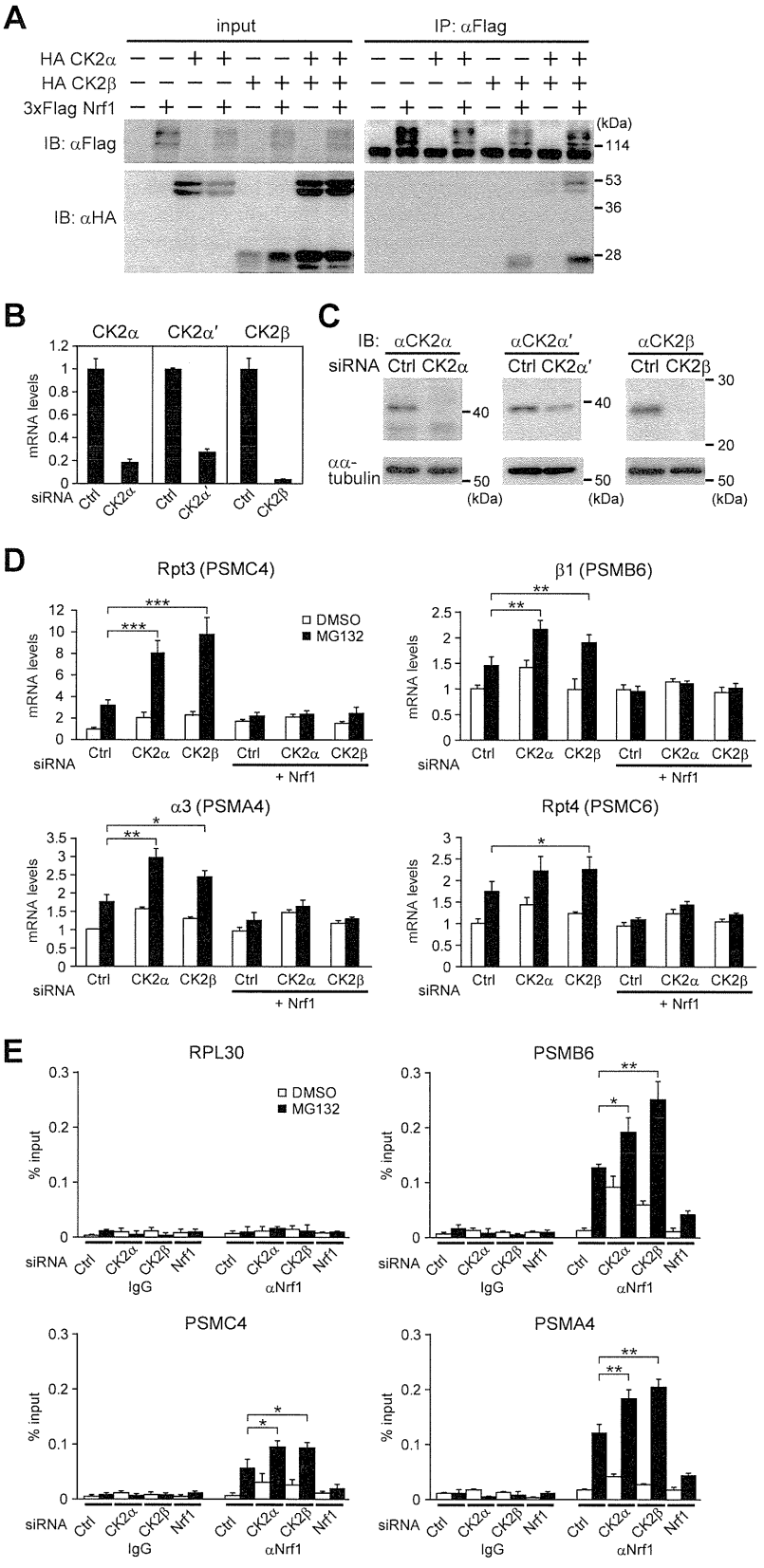

***In vitro* kinase assay.** Purified Nrf1 fragments were incubated with or without 100 ng of recombinant CK2α in kinase reaction buffer (50 mM Tris-HCl [pH 7.5], 200 mM NaCl, 10 mM $MgCl_2$, 15 mM β-glycerophosphate, 2 mM EGTA, 1 mM dithiothreitol [DTT], and 50 μM ATP) supplemented with 0.1 MBq of [γ-^{32}P]ATP for 15 min at 37°C. The reaction was stopped by the addition of SDS sample buffer. After resolution by SDS-PAGE, substrate phosphorylation was detected with a bioimaging analyzer (BAS-2500; Fujifilm).

Cycloheximide chase experiment. COS7 cells that were transfected with the plasmids indicated in the figures were treated with 20 μg/ml of cycloheximide, and the whole-cell extracts were prepared at the time points indicated in the figures and subjected to immunoblot analysis with the antibodies indicated in the figures.

Immunocytochemical staining. The cells were fixed with 4% formaldehyde for 10 min, washed twice with PBS, and permeabilized with 0.5% Triton X-100 in PBS for 5 min. The cells were washed twice with PBS and treated with the antibodies indicated in the figures for 1 h at room temperature. After the cells were washed three times with PBS, they were incubated with Alexa Fluor 488- or Alexa Fluor 546-conjugated secondary antibodies (Invitrogen) for 30 min at room temperature. The nuclei were stained with 4′,6′-diamidino-2-phenylindole (DAPI). After the cells were washed three times with PBS, they were sealed with a drop of fluorescence mounting medium (Dako). Fluorescent images were captured with an Olympus LX71 fluorescence microscope.

RESULTS

Nrf1 regulates the expression of almost all proteasome subunits and several proteasome-related genes. We first evaluated the importance of Nrf1 in the transcriptional induction of proteasome subunits and proteasome-related genes upon inhibition of the proteasome in HeLa cells. To this end, HeLa cells were treated with the proteasome inhibitor MG132 for 16 h in the presence or absence of siRNA that targets Nrf1. The Nrf1 mRNA expression level was significantly repressed by the Nrf1-specific siRNA (Fig. 1A). MG132 stabilized the Nrf1 protein as previously reported (17–19), and the siRNA-mediated knockdown of Nrf1 efficiently suppressed the accumulation of Nrf1 protein (Fig. 1B). Upon inhibition of the proteasome, Nrf1 is reported to stimulate the expression of a large set of proteasome subunit genes and the proteasome maturation factor POMP (18). Thus, we first examined the mRNA expression profiles of all the proteasome subunits and well-characterized proteasome-related genes. We found that most of the proteasome subunit genes were upregulated by MG132 in an Nrf1-dependent manner (Fig. 1C and D) and that the expression of almost all the base and lid subunit genes was significantly induced by proteasome inhibition in HeLa cells. In addition, among the many proteasome-related genes, the proteasome activator PA200, the proteasome-associated deubiquitinating enzyme Usp14, and POMP were markedly upregulated by MG132 in an Nrf1-dependent manner (Fig. 1C and D). These results reemphasize the importance of Nrf1 in the strong coordination of proteasome biogenesis. A time profile of proteasome subunit gene expression was correlated with that of Nrf1 accumulation in cells that were treated with MG132 (Fig. 1B and E).

It has been reported that dysfunction of the proteasome leads to the induction of molecular chaperones and several autophagy-related genes, including Hsp70, p62/SQSTM1, and Bag3 (24–26). These genes contribute to protein quality control and the activation of selective autophagy, another degradation pathway for ubiquitinated proteins (27, 28). We examined whether Nrf1 is involved in the expression of autophagy-related genes that are induced by proteasome inhibition. Treatment of the cells with MG132 significantly induced these genes, and knockdown of Nrf1 had little impact on this induction (Fig. 1D and data not shown). We also examined the expression of other candidate genes for Nrf1 targets, GSTA4 and NQO1, which are well-known ARE-regulated genes. As a result, expression of GSTA4 but not NQO1 was induced by MG132 in an Nrf1-dependent manner (Fig. 1E). These results indicate that, upon proteasome inhibition, Nrf1 specifically upregulates proteasome-related genes along with a subset of antioxidant response genes. As expression of several proteasome genes was also induced in an Nrf1-dependent manner in another human cell line, MCF10A, it is likely that Nrf1-dependent induction of proteasome genes is a general mechanism utilized by various types of cells, although there is some variation among cell lines in response to proteasome inhibition (data not shown).

Identification of CK2 as a suppressor of Nrf1-mediated transcription. It is conceivable that regulating the transcriptional activity of Nrf1 is of critical importance in controlling cellular proteasome activity. To understand regulatory mechanisms of Nrf1 activity, we conducted a mass spectrometric analysis and identified a wide variety of proteins as Nrf1-binding proteins (see Table S1 in the supplemental material) (19). We focused on the protein kinase CK2 because protein kinases are often the critical regulators for diverse transcription factors. CK2 was the only protein kinase identified in our analysis, and both the catalytic α subunit and the regulatory β subunit of CK2 were identified (see Tables S1 and S2 in the supplemental material). CK2 is known to form a heterotetrameric complex composed of two α (and/or α′) subunits and two β subunits (29). To further investigate the interaction of Nrf1 with the CK2 holoenzyme, we performed coimmunoprecipitation assays with COS7 cells. The results clearly demonstrate that CK2β was coimmunoprecipitated with Nrf1

FIG 2 CK2 regulates the Nrf1-dependent expression of proteasome genes. (A) Physical interaction of Nrf1 with CK2. Whole-cell extracts of COS7 cells expressing 3×Flag-tagged Nrf1 (3×Flag Nrf1), HA-tagged CK2α (HA CK2α), and HA CK2β were subjected to immunoprecipitation (IP) with anti-Flag antibody (αFlag), followed by immunoblot (IB) analysis with the indicated antibodies. (B) siRNA-mediated knockdown of CK2 subunits. HeLa cells were transfected with the indicated siRNAs. The mRNA expression levels of the indicated genes were determined by real-time quantitative PCR. The values were normalized to 18S rRNA values and presented as the means plus SD ($n = 3$). (C) The siRNA-mediated knockdown of CK2α, CK2α′, and CK2β was determined by immunoblot analysis. (D) Knockdown of the CK2 subunits enhances the Nrf1-dependent induction of proteasome genes. HeLa cells transfected with control (Ctrl), both CK2α and α′ (CK2α), or CK2β siRNA were treated with Nrf1 siRNA (+ Nrf1) or left untreated and treated with DMSO or 1 μM MG132 for 16 h. The mRNA expression levels were determined by real-time quantitative PCR analysis. The values were normalized to 18S rRNA values and presented as the means plus SD ($n = 3$). Values that are significantly different are indicated by asterisks and bars as follows: *, $P < 0.05$; **, $P < 0.01$; ***, $P < 0.001$. (E) Knockdown of the CK2 subunits enhanced the recruitment of Nrf1 to the AREs of proteasome gene promoters. HeLa cells were transfected with the indicated siRNAs and treated with DMSO or 1 μM MG132 for 16 h. The cells were subjected to chromatin immunoprecipitation (ChIP) analysis using normal rabbit IgG (IgG) or anti-Nrf1 antibody (αNrf1). The recruitment of Nrf1 to the AREs of *PSMB6*, *PSMC4*, and *PSMA4* was determined by real-time quantitative PCR. The promoter region of *RPL30* served as a negative control. The values were presented as the means plus SD ($n = 3$). Values that are significantly different are indicated by asterisks and bars as follows: *, $P < 0.05$; **, $P < 0.01$.

(Fig. 2A). Of note, CK2α was coimmunoprecipitated with Nrf1 only in the presence of CK2β (Fig. 2A). Thus, Nrf1 may bind to the CK2 holoenzyme through its regulatory β subunit. To examine whether CK2 regulates the transcriptional activity of Nrf1, we assessed the effect of an siRNA-mediated knockdown of the CK2 subunits on the Nrf1-dependent expression of the proteasome subunit genes. siRNAs for CK2α, CK2α′, a paralogous isoform of CK2α, and CK2β efficiently downregulated the expression of their target mRNAs (Fig. 2B). Efficient knockdown of CK2α, CK2α′, and CK2β was also confirmed by Western blotting (Fig. 2C). The siRNA-mediated knockdown of both CK2α and CK2α′ enhanced the MG132-induced expression of proteasome subunit genes such as *PSMC4*, *PSMB6*, *PSMA4*, and *PSMC6* (Fig. 2D). Knockdown of CK2β had similar effects on the expression of these genes (Fig. 2D). These enhancements were not observed when Nrf1 was downregulated simultaneously by siRNA (Fig. 2D). These results indicate that CK2 suppresses the Nrf1-dependent expression of proteasome subunit genes that are induced by proteasome inhibition. To further evaluate whether Nrf1 mediates the effect of CK2 knockdown on the transcription of proteasome genes, we performed chromatin immunoprecipitation (ChIP) assays using an anti-Nrf1 antibody. We examined the recruitment of Nrf1 to the AREs, which are located in the proximal promoter of *PSMC4* and *PSMB6* and in the first intron of *PSMA4* (16, 17). siRNA-mediated knockdown of CK2α and CK2β significantly augmented the recruitment of Nrf1 to the AREs, both with and without MG132 treatment (Fig. 2E; see Discussion). The 5′-upstream region of *RPL30* served as a negative control of Nrf1 binding. As siRNA-mediated knockdown of Nrf1 markedly decreased the amount of precipitated ARE regions of the proteasome subunit promoters (Fig. 2E), the observed ChIP signals should reflect Nrf1-ARE binding. These data collectively indicate that CK2 suppresses the transcriptional activity of Nrf1 by regulating the recruitment of Nrf1 to its target AREs.

The Nrf1-mediated transcriptional regulation of the proteasome subunit genes should control the total cellular proteasome activity. To investigate the effect of a CK2 knockdown on the detailed time profile of proteasome activity under conditions of proteasome inhibition, we performed real-time monitoring of proteasome activity in living cells. We utilized a ubiquitin-fused luciferase reporter (Ub-FL) as the indicator of endogenous proteasome activity (20). In this system, high reporter activity corresponds to low proteasome activity. The addition of the proteasome inhibitor epoxomicin resulted in a gradual increase of the reporter activity, which was greatly enhanced by siRNA-mediated knockdown of Nrf1 (Fig. 3A). In contrast, the knockdown of either CK2α or CK2β suppressed the epoxomicin-induced stabilization of the reporter protein (Fig. 3A). Similar results were obtained by measuring the properly normalized reporter activity in cell lysates that were prepared 16 h after the addition of epoxomicin (Fig. 3B). We also measured endogenous proteasome activity by using a luminogenic substrate Suc-LLVY-aminoluciferin for the chymotrypsin-like activity. The result demonstrates that Nrf1 knockdown cells show lower proteasome activity than control cells 24 h after epoxomicin treatment (Fig. 3C). On the other hand, CK2α or CK2β knockdown cells show slightly higher proteasome activity than control cells, although the difference in proteasome activity is moderate compared with the results in Fig. 3A and B. These results suggest that CK2-mediated suppression of

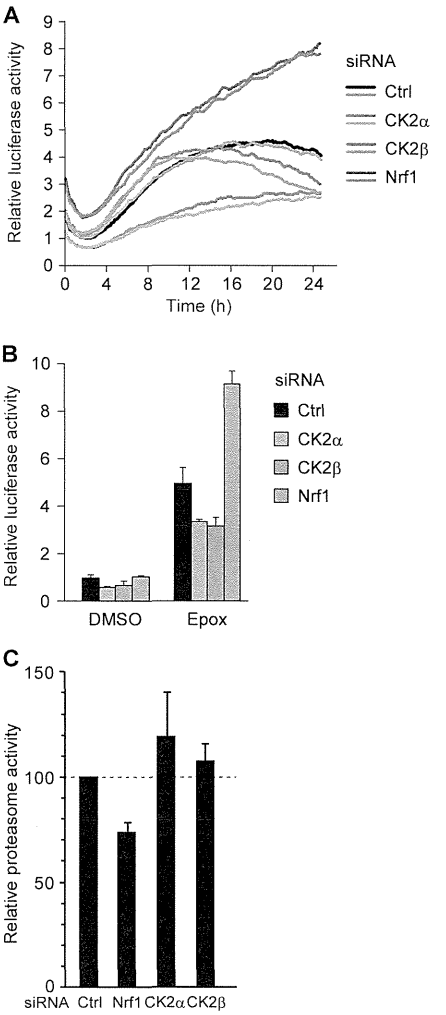

FIG 3 Knockdown of the CK2 subunits or Nrf1 affects degradation of ubiquitinated proteins. (A) HeLa cells transfected with the Ub-FL reporter plasmid and the indicated siRNAs were treated with 0.1 mM D-luciferin. Real-time monitoring of the reporter activity was performed using a photomultiplier. Epoxomicin was added to the culture medium 1 to 2 h after the start of measurement. The darker and lighter lines indicate duplicate traces of two independent samples. Representative data are shown. (B) HeLa cells transfected with the Ub-FL reporter plasmid, the control *Renilla* luciferase reporter, and the indicated siRNAs were treated with DMSO or 10 nM epoxomicin (Epox) with D-luciferin for 16 h. The cells were lysed and subjected to a luciferase assay. The values were normalized to *Renilla* luciferase activity values and presented as the means plus SD ($n = 3$). (C) HeLa cells transfected with control (Ctrl), Nrf1, CK2α, or CK2β siRNA were treated with 10 nM epoxomicin for 24 h. The proteasome activity was determined by using a luminogenic substrate Suc-LLVY-aminoluciferin for the chymotrypsin-like activity. The values were shown as the percent changes of proteasome activity over the control siRNA-treated cells (means plus SD, $n = 9$).

Nrf1 activity leads to the downregulation of proteasome activity in cells.

CK2 phosphorylates Nrf1 at a specific serine residue. Next, we focused on the underlying mechanisms of the CK2 regulation of Nrf1. We assumed that CK2 directly phosphorylates Nrf1 and regulates its transcriptional activity. To test this hypothesis, we performed an *in vitro* kinase assay using recombinant CK2α and a

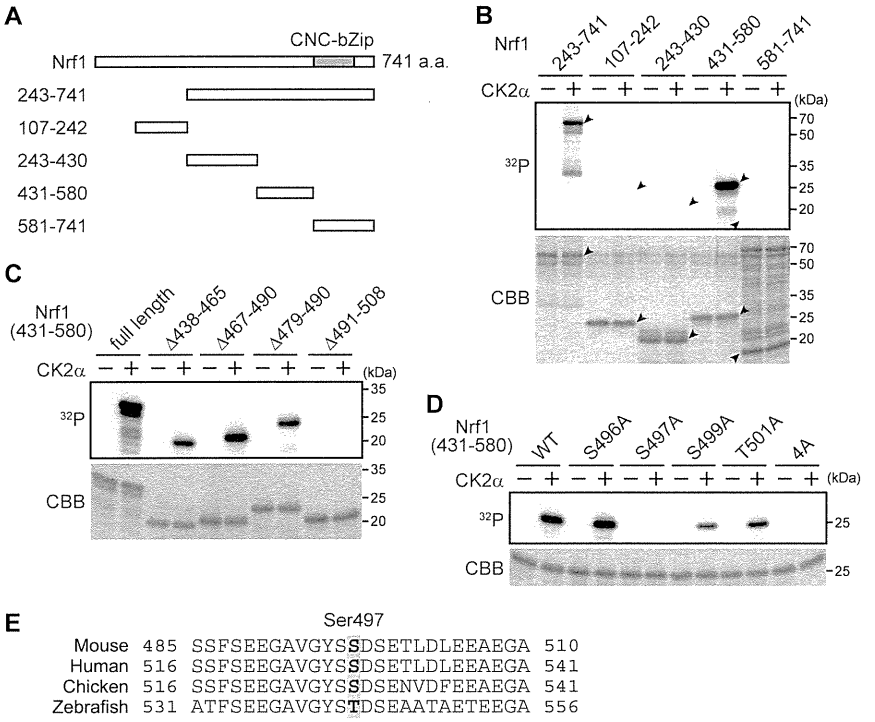

FIG 4 CK2 phosphorylates Nrf1 at Ser 497. (A) Schematic structures of the Nrf1 fragments. a.a., amino acids. (B) CK2 phosphorylates residues 431 to 580 of Nrf1. The purified Nrf1 fragments were incubated in the presence of [γ-^{32}P]ATP with (+) or without (−) recombinant CK2α. The autoradiograph was analyzed with a phosphorimager. The indicated input proteins were analyzed by Coomassie brilliant blue (CBB) staining. The positions of input proteins are indicated by black arrowheads. (C) CK2 phosphorylates residues 491 to 501 of Nrf1. The Nrf1 fragments (residues 431 to 580) with the indicated internal deletions were subjected to an *in vitro* phosphorylation assay. (D) CK2 phosphorylates Ser 497 of Nrf1. The Nrf1 fragments (residues 431 to 580) with the indicated point mutations were subjected to an *in vitro* phosphorylation assay. WT, wild type; 4A, all four of the candidate serine/threonine residues were replaced by alanine. (E) Conservation of Nrf1 sequences among the species around the CK2-mediated phosphorylation site.

series of Nrf1 fragments (Fig. 4A). Among the constructed fragments, Nrf1 (residues 431 to 580) was specifically phosphorylated by CK2α (Fig. 4B). Additional experiments narrowed the phosphorylation site to a small region (residues 491 to 508) of Nrf1 (Fig. 4C). We introduced an alanine substitution at each of the four candidate phosphoacceptor sites (Ser 496, Ser 497, Ser 499, and Thr 501). Of the constructed mutants, only the Ser 497 to Ala (S497A) mutant was not phosphorylated by CK2α *in vitro* (Fig. 4D). Thus, we concluded that Ser 497 of Nrf1 is the primary target for phosphorylation by CK2α *in vitro* (Fig. 4E).

The CK2 phosphorylation site mutant enhances the transcriptional activity of Nrf1. To investigate the effect of the CK2-mediated phosphorylation of Nrf1, we compared the transcriptional activity of the S497A mutant with wild-type Nrf1 (Nrf1-WT). We used a luciferase reporter that was driven by three tandem copies of the ARE from the PSMA4 promoter (17). Forced expression of Nrf1 increased the reporter activity in a dose-dependent manner (Fig. 5A). Notably, the S497A mutant exhibited enhanced transcriptional activity compared to wild-type Nrf1 (Fig. 5A). Similar results were obtained with the reporter assay using pRBGP2 luciferase reporter that was driven by three tandem copies of the MARE (Fig. 5A) (21). Furthermore, forced expression of the Nrf1-S497A mutant increased expression of endogenous proteasome genes such as PSMC4 and PSMA4 much more than Nrf1-WT, although expression of PSMB6 did not increase significantly (Fig. 5B). As the steady-state level and the degradation rates of these proteins were comparable (Fig. 5C), the enhanced activity of the S497A mutant is not merely due to the elevated expression and/or stabilization of the Nrf1 proteins. In addition, there was no difference in the subcellular localization and physical interaction with MafK, a heterodimerization partner of Nrf1, between wild-type Nrf1 and the S497A mutant (data not shown). We next examined whether the enhanced transcriptional activity of the S497A mutant could affect endogenous proteasome activity. The Ub-FL reporter plasmid with either wild-type Nrf1 or the S497A mutant expression plasmid was transfected into HeLa cells, and the reporter activity was monitored in cells treated with epoxomicin. The forced expression of wild-type Nrf1 prevented the increase in reporter activity that was induced by epoxomicin in a dose-dependent manner (Fig. 5D). This result suggests that the upregulation of the proteasome activity by the Nrf1-mediated induction of proteasome expression confers tolerance for proteasome inhibition on cells. Importantly, compared to wild-type Nrf1, the S497A mutant had a greater ability to prevent the increase in reporter activity (Fig. 5D). Similar results were obtained by measuring the properly normalized reporter activity in cell lysates prepared 16 h after the addition of epoxomicin (Fig. 5E). These results clearly demonstrate that the CK2 phosphorylation site mutant of Nrf1 has a greater ability to upregulate proteasome expression and activity than wild-type Nrf1. To evaluate the im-

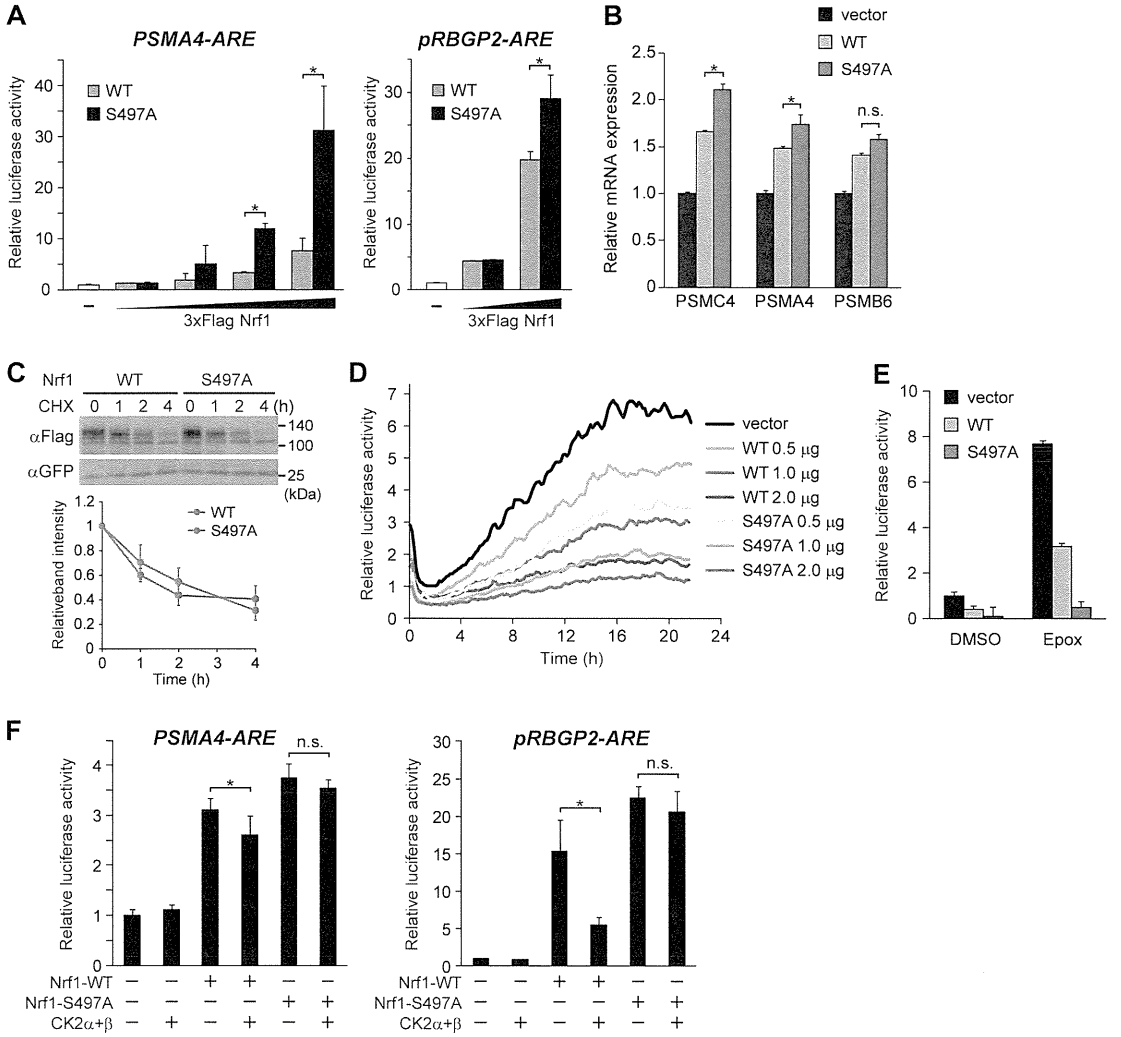

FIG 5 The Nrf1-S497A mutant has enhanced transcriptional activity and prevents the accumulation of ubiquitinated proteins. (A) The S497A mutant has enhanced transcriptional activity. COS7 cells transfected with either wild-type (WT) plasmid or S497A mutant plasmid in combination with a luciferase reporter containing three tandem copies of the AREs of *PSMA4* or a pRBGP2 reporter. The levels of luciferase activity were normalized to the *Renilla* luciferase activity of an internal control pRL-TK and presented as the means plus SD ($n = 3$). Values that are significantly different ($P < 0.05$) are indicated by a bar and asterisk. (B) The S497A mutant upregulates expression of endogenous proteasome genes. HeLa cells were transfected with either wild-type (WT) or S497A mutant plasmid. The mRNA expression levels were determined by real-time quantitative PCR analysis. The values were normalized to 18S rRNA values and presented as the means plus SD ($n = 5$). Values that are significantly different ($P < 0.05$) are indicated by a bar and asterisk. Values that are not significantly different are indicated by a bar labeled n.s. (C) Protein stability is comparable in the wild type and the S497A mutant. COS7 cells transfected with the expression plasmid for the wild-type 3×Flag Nrf1 protein or the S497A mutant of 3×Flag Nrf1 in combination with the GFP expression plasmid were treated with 20 μg/ml cycloheximide (CHX). The cells were lysed at the indicated time points and subjected to immunoblot analysis with anti-Flag or anti-GFP antibodies. The data were normalized to cotransfected GFP values and are presented as the means ± standard errors (SE) ($n = 3$). (D and E) The S497A mutant has a greater ability to repress the accumulation of ubiquitinated proteins than wild-type Nrf1. (D) HeLa cells transfected with the Ub-FL reporter plasmid in combination with the indicated amount of wild-type or S497A mutant Nrf1 plasmid were treated with 10 nM epoxomicin and D-luciferin. Real-time monitoring of the reporter activity was performed using a photomultiplier, and representative data are shown. (E) HeLa cells transfected with the Ub-FL reporter plasmid and the control *Renilla* luciferase reporter in combination with the wild-type or S497A mutant plasmid were treated with DMSO or 10 nM epoxomicin with D-luciferin for 16 h. The cells were lysed and subjected to a luciferase assay. The values were normalized to the values for *Renilla* luciferase activity and presented as the means plus SD ($n = 3$). (F) CK2 suppresses the transcriptional activity of Nrf1-WT but not that of the Nrf1-S497A mutant. COS7 cells were transfected with the indicated plasmids in combination with the *PSMA4*-ARE reporter or a pRBGP2 reporter. The levels of luciferase activity were normalized to the values for *Renilla* luciferase activity of an internal control pRL-TK and presented as the means plus SD ($n = 3$). Statistical significance is indicated as follows: *, $P < 0.05$; n.s., not significant.

portance of phosphorylation at Ser 497 in the regulation by CK2, we examined whether CK2 affects the transcriptional activity of Nrf1-WT and Nrf1-S497A. The results demonstrate that CK2 suppresses the PSMA4 reporter activity induced by Nrf1-WT but not by the Nrf1-S497A mutant (Fig. 5F, left graph). Similar results were obtained using the pRBGP2 reporter (Fig. 5F, right graph). These results collectively suggest that CK2 suppresses the transcriptional activity of Nrf1 via phosphorylation of Nrf1 at Ser 497.

The CK2 phosphorylation site mutant of Nrf1 suppresses the formation of p62-positive inclusion bodies. Proteasome dysfunction is associated with the formation of juxtanuclear inclusion bodies such as aggresomes (1). These inclusion bodies contain p62 and function to sequester unfolded and misfolded proteins that could not be degraded by the proteasome (30). The phosphorylation state of Ser 497 of Nrf1 may affect the efficiency of the formation of such inclusion bodies. To assess this possibility, we examined the effect of forced expression of the S497A mutant of Nrf1 on the formation of p62-positive inclusion bodies. Treatment of cells with epoxomicin led to the formation of p62-positive juxtanuclear inclusion bodies in HeLa cells (Fig. 6A). Similar results were obtained when MG132 was used instead of epoxomicin (data not shown). Strikingly, the siRNA-mediated knockdown of Nrf1 markedly enhanced the inclusion body formation (Fig. 6A). This result indicates that Nrf1 plays an important role in preventing the formation of juxtanuclear inclusion bodies. These p62-positive inclusion bodies were also ubiquitin positive, indicating the accumulation of ubiquitinated proteins (Fig. 6B). Knockdown of Nrf1 did not affect the total amount of p62 but caused an increase in the autophagic marker LC3-II (Fig. 6C). This finding suggests that the downregulation of Nrf1 leads to the accumulation of autophagosomes that are involved in an alternative degradation pathway for misfolded proteins. We tested the effect of Nrf1 overexpression on inclusion body formation. Forced expression of wild-type Nrf1 decreased the efficiency of formation of the p62-positive juxtanuclear inclusion bodies that were induced by epoxomicin (Fig. 6D). Importantly, forced expression of the S497A mutant reduced inclusion body formation more effectively than that of wild-type Nrf1 (Fig. 6D). These results suggest that the phosphorylation state of Ser 497 affects the formation efficiency of the p62-positive juxtanuclear inclusion bodies that are induced by proteasome inhibition.

DISCUSSION

Significance of CK2 as a regulator of Nrf1 transcriptional activity. In this study, we demonstrate that CK2 interacts with and phosphorylates Nrf1 and suppresses its transcriptional activity, thereby regulating the expression of proteasome subunits. Nrf1 is localized to the endoplasmic reticulum (ER) membrane and is constitutively degraded by the proteasome under normal conditions (18, 19). Inhibition or dysfunction of the proteasome may induce the stabilization and nuclear translocation of Nrf1 proteins. Our results have implicated CK2 in the regulatory mechanisms of Nrf1 activity. Given that knockdown of the CK2 subunits facilitates the recruitment of Nrf1 to the AREs of their promoters and increases the expression of Nrf1 target genes even without proteasome inhibition (Fig. 2D and E), CK2 may suppress the transcriptional activity of Nrf1 and thus prevent the unnecessary expression of Nrf1 target genes under physiological conditions. As we have no data indicating that phosphorylation of Ser 497 is altered in response to proteasome inhibition, it remains to be elucidated whether CK2-mediated phosphorylation of Nrf1 is regulated during Nrf1 activation. Our preliminary data demonstrate that the expression of CK2α is reduced upon inhibition of the proteasome (data not shown). Although the mechanism underlying the decrease in CK2α expression is unclear, it is possible that Nrf1 phosphorylation is decreased upon proteasome inhibition, resulting in efficient transcriptional activation of stabilized Nrf1 proteins.

Nrf1 exists as multiple isoforms, including TCF11 (transcription factor 11), a longer isoform found in humans (31). The regulatory mechanism for TCF11 might differ from that of Nrf1, as TCF11 has the nuclear export signal that is not present in Nrf1. In this study, we used the expression plasmid for mouse Nrf1 but not the expression plasmid for TCF11. Thus, it remains to be elucidated in future studies whether human TCF11 can be regulated by CK2 and whether there is any difference in CK2-mediated regulation between mouse Nrf1 and human TCF11. In addition to a known proteasome-mediated regulation of Nrf1 activity, we propose that CK2-mediated phosphorylation of Nrf1 acts as another layer of Nrf1 regulation to fine-tune its transcriptional activity.

Effect of CK2-mediated direct phosphorylation of Nrf1. The phosphorylation of Nrf1 Ser 497 is likely to enhance its transcriptional activity but not affect its stability, subcellular localization, or ability to bind MafK proteins. Our data indicate that Ser 497 has an important role in CK2-dependent suppression of Nrf1 transcriptional activity. Given that CK2 knockdown enhances the recruitment of Nrf1 to its target AREs, it is likely that CK2-mediated phosphorylation of Ser 497 controls the recruitment of Nrf1 to the AREs of the target promoters. However, it remains to be investigated how phosphorylation of Ser 497 suppresses Nrf1 recruitment. As Ser 497 resides in the Neh6-like domain and are located next to the CNC-bZip domain, phosphorylation may induce a conformational change of the Nrf1 protein, compromising its binding to the target DNA.

Ser 497 of mouse Nrf1 is conserved in mouse Nrf2 (Ser 365), but it is not known whether CK2 can phosphorylate Nrf2 at Ser 365. It has been reported that Nrf2 is phosphorylated by CK2 and that this phosphorylation regulates the transcriptional activity of Nrf2 (32, 33). The effect of the CK2-mediated phosphorylation on Nrf2 activity is controversial, but several reports have shown that CK2 inhibition results in Nrf2 inactivation (32, 34, 35). The CK2-mediated phosphorylation of Nrf2 facilitates its nuclear translocation and the upregulation of Nrf2 target gene expression. Thus, it seems likely that the role of CK2-dependent regulation in Nrf2 may be different from that in Nrf1.

The CK2-Nrf1 axis as a new therapeutic target for diseases associated with proteasome dysfunction. The regulation of proteasome activity is an established strategy for cancer treatment, and it is expected to be a promising approach to ameliorate some age-related disorders, such as neurodegenerative diseases. Supporting this notion, a previous study has demonstrated that a small-molecule inhibitor of USP14, a proteasome-associated deubiquitinating enzyme, increases the proteasome activity and enhances the degradation of several neurodegenerative disease-associated proteins such as tau and TDP-43 (36). Thus, the upregulation of proteasome activity should alleviate the accumulation of aggregate-prone proteins. In addition, it has been reported that overexpression of a proteasome subunit gene increases proteasome activity, decreases the accumulation of ubiquitinated proteins, and ameliorates the response to oxidative stress (37–39). Therefore, the fact that Nrf1 regulates the expression of most of the proteasome subunit genes may provide a new approach, transcriptional upregulation of the proteasome, to treat human diseases associated with the accumulation of abnormal proteins. Our findings that Nrf1-S497A exerts a more significant effect on the inhibition of p62-positive inclusion body formation than wild-type Nrf1 does strongly suggest that the CK2-mediated phosphor-

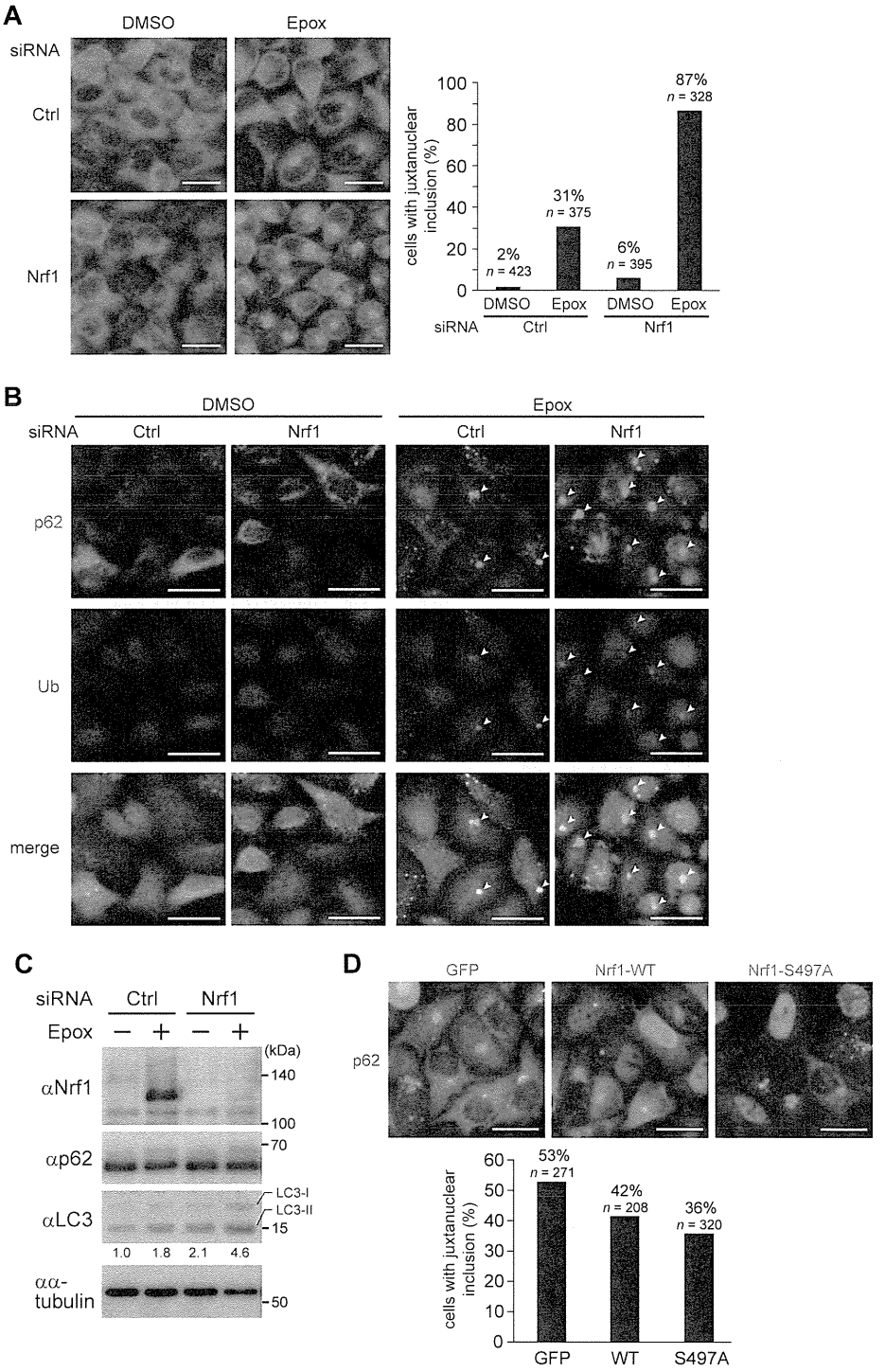

FIG 6 Nrf1 has the ability to ameliorate the formation of p62-positive inclusion bodies in HeLa cells. (A) Knockdown of Nrf1 causes enhanced formation of p62-positive inclusion bodies. HeLa cells transfected with control (Ctrl) or Nrf1 siRNA were treated with DMSO or 10 nM epoxomicin for 24 h. The cells were immunostained with anti-p62 antibody, and the percentage of cells containing juxtanuclear inclusion bodies were calculated. Bars, 50 μm. (B) p62-positive inclusion bodies formed by proteasome inhibition are ubiquitin positive. HeLa cells transfected with control (Ctrl) or Nrf1 siRNA were treated with DMSO or 10 nM epoxomicin for 24 h. The cells were immunostained with anti-p62 (green) and antiubiquitin (red) antibodies. Juxtanuclear inclusion bodies stained with both antibodies are indicated by small white arrowheads. Bars, 50 μm. (C) The cells treated as in panel A were lysed and subjected to immunoblot analysis with the indicated antibodies. The relative band intensities of LC3-II were quantified and normalized to α-tubulin values. (D) The S497A mutant has a greater ability to decrease the formation of p62-positive juxtanuclear inclusion bodies than wild-type Nrf1. HeLa cells transfected with the expression plasmid for GFP or wild-type or the S497A mutant of 3×Flag Nrf1 were treated with DMSO or 10 nM epoxomicin for 24 h. The cells were immunostained with anti-Flag and anti-p62 antibodies, and the percentage of cells containing juxtanuclear inclusion bodies out of total GFP- or 3×Flag Nrf1-expressing cells were calculated. Bars, 50 μm.

ylation of Nrf1 is one of the potential targets for treating proteinopathies such as neurodegenerative diseases.

CK2 has an array of substrate proteins and functions in diverse cellular processes, including cell growth and proliferation (40, 41). Recent studies have also implicated CK2 in neuronal functions and the progression of neurodegenerative diseases (42, 43). It has been reported that CK2 phosphorylates several neurodegenerative disease-related proteins, such as α-synuclein, synphilin-1, and apolipoprotein E, to enhance aggregate formation (44–46). Thus, the regulation of CK2 activity may represent a possible target for therapeutic intervention. Indeed, CK2 inhibition has been shown to exert a protective effect on neurons (44, 47, 48). In contrast, a recent report has shown that CK2 phosphorylates p62 and stimulates the clearance of protein aggregates via the autophagy-lysosome pathway (49). This finding raises the possibility that CK2 inhibition or knockdown results in the impairment of aggregate clearance. Therefore, there seem to be pros and cons to modulating CK2 activity with regard to ameliorating proteinopathies. Nevertheless, our data strongly suggest that the CK2-mediated regulation of Nrf1 can be a novel target for the treatment of diseases associated with proteasome dysfunction.

ACKNOWLEDGMENTS

We are grateful to David Piwnica-Worms and Raymond J. Deshaies for the Ub-FL plasmid and the 3xPSMA4-ARE-Luc plasmid, respectively. We also thank Noriko Noguchi and Akiko Matsumoto for research support.

This work was supported in part by grants-in-aid (A.K. and Y.T.) and the Strategic Research Foundation at Private Universities (2012 to 2016) (A.K.) from the Ministry of Education, Sports, Science and Technology, the Mochida Memorial Foundation (A.K.), the Naito Foundation (A.K.), the Suzuken Memorial Foundation (A.K.), the Takeda Science Foundation (A.K.), the Uehara Memorial Foundation (A.K.), Astellas Foundation for Research on Metabolic Disorders (A.K.), and the Inamori Foundation (Y.T.).

REFERENCES

1. Kopito RR. 2000. Aggresomes, inclusion bodies and protein aggregation. Trends Cell Biol. 10:524–530.
2. Ross CA, Poirier MA. 2004. Protein aggregation and neurodegenerative disease. Nat. Med. 10:S10–S17.
3. Strnad P, Zatloukal K, Stumptner C, Kulaksiz H, Denk H. 2008. Mallory-Denk-bodies: lessons from keratin-containing hepatic inclusion bodies. Biochim. Biophys. Acta 1782:764–774.
4. Glickman MH, Ciechanover A. 2002. The ubiquitin-proteasome proteolytic pathway: destruction for the sake of construction. Physiol. Rev. 82: 373–428.
5. Levine B, Kroemer G. 2008. Autophagy in the pathogenesis of disease. Cell 132:27–42.
6. Mizushima N, Levine B, Cuervo AM, Klionsky DJ. 2008. Autophagy fights disease through cellular self-digestion. Nature 451:1069–1075.
7. Rubinsztein DC. 2006. The roles of intracellular protein-degradation pathways in neurodegeneration. Nature 443:780–786.
8. Kobayashi M, Yamamoto M. 2006. Nrf2-Keap1 regulation of cellular defense mechanisms against electrophiles and reactive oxygen species. Adv. Enzyme Regul. 46:113–140.
9. Sykiotis GP, Bohmann D. 2010. Stress-activated cap'n'collar transcription factors in aging and human disease. Sci. Signal. 3:re3. doi:10.1126/scisignal.3112re3.
10. Chan JY, Kwong M, Lu R, Chang J, Wang B, Yen TS, Kan YW. 1998. Targeted disruption of the ubiquitous CNC-bZIP transcription factor, Nrf-1, results in anemia and embryonic lethality in mice. EMBO J. 17: 1779–1787.
11. Kim J, Xing W, Wergedal J, Chan JY, Mohan S. 2010. Targeted disruption of nuclear factor erythroid-derived 2-like 1 in osteoblasts reduces bone size and bone formation in mice. Physiol. Genomics 40:100–110.
12. Ohtsuji M, Katsuoka F, Kobayashi A, Aburatani H, Hayes JD, Yamamoto M. 2008. Nrf1 and Nrf2 play distinct roles in activation of antioxidant response element-dependent genes. J. Biol. Chem. 283: 33554–33562.
13. Xing W, Singgih A, Kapoor A, Alarcon CM, Baylink DJ, Mohan S. 2007. Nuclear factor-E2-related factor-1 mediates ascorbic acid induction of osterix expression via interaction with antioxidant-responsive element in bone cells. J. Biol. Chem. 282:22052–22061.
14. Xu Z, Chen L, Leung L, Yen TS, Lee C, Chan JY. 2005. Liver-specific inactivation of the Nrf1 gene in adult mouse leads to nonalcoholic steatohepatitis and hepatic neoplasia. Proc. Natl. Acad. Sci. U. S. A. 102:4120–4125.
15. Kobayashi A, Tsukide T, Miyasaka T, Morita T, Mizoroki T, Saito Y, Ihara Y, Takashima A, Noguchi N, Fukamizu A, Hirotsu Y, Ohtsuji M, Katsuoka F, Yamamoto M. 2011. Central nervous system-specific deletion of transcription factor Nrf1 causes progressive motor neuronal dysfunction. Genes Cells 16:692–703.
16. Lee CS, Lee C, Hu T, Nguyen JM, Zhang J, Martin MV, Vawter MP, Huang EJ, Chan JY. 2011. Loss of nuclear factor E2-related factor 1 in the brain leads to dysregulation of proteasome gene expression and neurodegeneration. Proc. Natl. Acad. Sci. U. S. A. 108:8408–8413.
17. Radhakrishnan SK, Lee CS, Young P, Beskow A, Chan JY, Deshaies RJ. 2010. Transcription factor Nrf1 mediates the proteasome recovery pathway after proteasome inhibition in mammalian cells. Mol. Cell 38:17–28.
18. Steffen J, Seeger M, Koch A, Kruger E. 2010. Proteasomal degradation is transcriptionally controlled by TCF11 via an ERAD-dependent feedback loop. Mol. Cell 40:147–158.
19. Tsuchiya Y, Morita T, Kim M, Iemura S, Natsume T, Yamamoto M, Kobayashi A. 2011. Dual regulation of the transcriptional activity of Nrf1 by β-TrCP- and Hrd1-dependent degradation mechanisms. Mol. Cell. Biol. 31:4500–4512.
20. Luker GD, Pica CM, Song J, Luker KE, Piwnica-Worms D. 2003. Imaging 26S proteasome activity and inhibition in living mice. Nat. Med. 9:969–973.
21. Igarashi K, Itoh K, Motohashi H, Hayashi N, Matuzaki Y, Nakauchi H, Nishizawa M, Yamamoto M. 1995. Activity and expression of murine small Maf family protein MafK. J. Biol. Chem. 270:7615–7624.
22. Igarashi K, Kataoka K, Itoh K, Hayashi N, Nishizawa M, Yamamoto M. 1994. Regulation of transcription by dimerization of erythroid factor NF-E2 p45 with small Maf proteins. Nature 367:568–572.
23. Miyata Y, Nishida E. 2005. CK2 binds, phosphorylates, and regulates its pivotal substrate Cdc37, an Hsp90-cochaperone. Mol. Cell. Biochem. 274: 171–179.
24. Kuusisto E, Suuronen T, Salminen A. 2001. Ubiquitin-binding protein p62 expression is induced during apoptosis and proteasomal inhibition in neuronal cells. Biochem. Biophys. Res. Commun. 280:223–228.
25. Wang HQ, Liu HM, Zhang HY, Guan Y, Du ZX. 2008. Transcriptional upregulation of BAG3 upon proteasome inhibition. Biochem. Biophys. Res. Commun. 365:381–385.
26. Zhou M, Wu X, Ginsberg HN. 1996. Evidence that a rapidly turning over protein, normally degraded by proteasomes, regulates hsp72 gene transcription in HepG2 cells. J. Biol. Chem. 271:24769–24775.
27. Gamerdinger M, Hajieva P, Kaya AM, Wolfrum U, Hartl FU, Behl C. 2009. Protein quality control during aging involves recruitment of the macroautophagy pathway by BAG3. EMBO J. 28:889–901.
28. Johansen T, Lamark T. 2011. Selective autophagy mediated by autophagic adapter proteins. Autophagy 7:279–296.
29. Niefind K, Guerra B, Ermakowa I, Issinger OG. 2001. Crystal structure of human protein kinase CK2: insights into basic properties of the CK2 holoenzyme. EMBO J. 20:5320–5331.
30. Komatsu M, Waguri S, Koike M, Sou YS, Ueno T, Hara T, Mizushima N, Iwata J, Ezaki J, Murata S, Hamazaki J, Nishito Y, Iemura S, Natsume T, Yanagawa T, Uwayama J, Warabi E, Yoshida H, Ishii T, Kobayashi A, Yamamoto M, Yue Z, Uchiyama Y, Kominami E, Tanaka K. 2007. Homeostatic levels of p62 control cytoplasmic inclusion body formation in autophagy-deficient mice. Cell 131:1149–1163.
31. Husberg C, Murphy P, Bjørgo E, Kalland KH, Kolstø AB. 2003. Cellular localisation and nuclear export of the human bZIP transcription factor TCF11. Biochim. Biophys. Acta 1640:143–151.
32. Apopa PL, He X, Ma Q. 2008. Phosphorylation of Nrf2 in the transcription activation domain by casein kinase 2 (CK2) is critical for the nuclear translocation and transcription activation function of Nrf2 in IMR-32 neuroblastoma cells. J. Biochem. Mol. Toxicol. 22:63–76.
33. Pi J, Bai Y, Reece JM, Williams J, Liu D, Freeman ML, Fahl WE, Shugar

D, Liu J, Qu W, Collins S, Waalkes MP. 2007. Molecular mechanism of human Nrf2 activation and degradation: role of sequential phosphorylation by protein kinase CK2. Free Radic. Biol. Med. 42:1797–1806.
34. Afonyushkin T, Oskolkova OV, Binder BR, Bochkov VN. 2011. Involvement of CK2 in activation of electrophilic genes in endothelial cells by oxidized phospholipids. J. Lipid Res. 52:98–103.
35. Ivanov AV, Smirnova OA, Ivanova ON, Masalova OV, Kochetkov SN, Isaguliants MG. 2011. Hepatitis C virus proteins activate NRF2/ARE pathway by distinct ROS-dependent and independent mechanisms in HUH7 cells. PLoS One 6:e24957. doi:10.1371/journal.pone.0024957.
36. Lee BH, Lee MJ, Park S, Oh DC, Elsasser S, Chen PC, Gartner C, Dimova N, Hanna J, Gygi SP, Wilson SM, King RW, Finley D. 2010. Enhancement of proteasome activity by a small-molecule inhibitor of USP14. Nature 467:179–184.
37. Chondrogianni N, Gonos ES. 2007. Overexpression of hUMP1/POMP proteasome accessory protein enhances proteasome-mediated antioxidant defence. Exp. Gerontol. 42:899–903.
38. Chondrogianni N, Tzavelas C, Pemberton AJ, Nezis IP, Rivett AJ, Gonos ES. 2005. Overexpression of proteasome beta5 assembled subunit increases the amount of proteasome and confers ameliorated response to oxidative stress and higher survival rates. J. Biol. Chem. 280:11840–11850.
39. Tonoki A, Kuranaga E, Tomioka T, Hamazaki J, Murata S, Tanaka K, Miura M. 2009. Genetic evidence linking age-dependent attenuation of the 26S proteasome with the aging process. Mol. Cell. Biol. 29:1095–1106.
40. Allende JE, Allende CC. 1995. Protein kinases. 4. Protein kinase CK2: an enzyme with multiple substrates and a puzzling regulation. FASEB J. 9:313–323.
41. Meggio F, Pinna LA. 2003. One-thousand-and-one substrates of protein kinase CK2? FASEB J. 17:349–368.
42. Blanquet PR. 2000. Casein kinase 2 as a potentially important enzyme in the nervous system. Prog. Neurobiol. 60:211–246.
43. Perez DI, Gil C, Martinez A. 2011. Protein kinases CK1 and CK2 as new targets for neurodegenerative diseases. Med. Res. Rev. 31:924–954.
44. Lee G, Tanaka M, Park K, Lee SS, Kim YM, Junn E, Lee SH, Mouradian MM. 2004. Casein kinase II-mediated phosphorylation regulates α-synuclein/synphilin-1 interaction and inclusion body formation. J. Biol. Chem. 279:6834–6839.
45. Okochi M, Walter J, Koyama A, Nakajo S, Baba M, Iwatsubo T, Meijer L, Kahle PJ, Haass C. 2000. Constitutive phosphorylation of the Parkinson's disease associated α-synuclein. J. Biol. Chem. 275:390–397.
46. Raftery M, Campbell R, Glaros EN, Rye KA, Halliday GM, Jessup W, Garner B. 2005. Phosphorylation of apolipoprotein-E at an atypical protein kinase CK2 PSD/E site in vitro. Biochemistry 44:7346–7353.
47. Chen-Roetling J, Li Z, Regan RF. 2008. Hemoglobin neurotoxicity is attenuated by inhibitors of the protein kinase CK2 independent of heme oxygenase activity. Curr. Neurovasc. Res. 5:193–198.
48. Moreno H, Yu E, Pigino G, Hernandez AI, Kim N, Moreira JE, Sugimori M, Llinás RR. 2009. Synaptic transmission block by presynaptic injection of oligomeric amyloid beta. Proc. Natl. Acad. Sci. U. S. A. 106:5901–5906.
49. Matsumoto G, Wada K, Okuno M, Kurosawa M, Nukina N. 2011. Serine 403 phosphorylation of p62/SQSTM1 regulates selective autophagic clearance of ubiquitinated proteins. Mol. Cell 44:279–289.

FEBS Letters 587 (2013) 2173–2178

FEBS Letters

journal homepage: www.FEBSLetters.org

LARP1 specifically recognizes the 3′ terminus of poly(A) mRNA

Kazuma Aoki [1], Shungo Adachi [1], Masae Homoto, Hideo Kusano, Katsuyuki Koike, Tohru Natsume *

Molecular Profiling Research Center for Drug Discovery(molprof), National Institute of Advanced Industrial Science and Technology (AIST), 2-4-7 Aomi, Koutou, Tokyo 135-0064, Japan

ARTICLE INFO

Article history:
Received 29 March 2013
Revised 8 May 2013
Accepted 9 May 2013
Available online 24 May 2013

Edited by Michael Ibba

Keywords:
RNA-directed immunoprecipitation
Proteomics
LAPP1
Poly(A) tail
5′TOP mRNA

ABSTRACT

A poly(A) tail functions in mRNA turnover and in facilitating translation as a ribonucleoprotein complex with poly(A) binding proteins (PABPs). However, factors that associate with the poly(A) tail other than PABPs have not been described. Using proteomics, we identified candidate proteins that interact to the 3′ terminus of the poly(A) tail. Among these proteins, we focused on La motif-related protein 1 (LARP1) and found that LARP1 specifically recognizes the 3′ termini of normal poly(A) tails. We also reveal that LARP1 stabilizes multiple mRNAs carrying 5′ terminal oligopyrimidine tract (5′TOP). Our findings suggest that LARP1 may be involved in the post-transcriptional regulation of gene expression, at least in several 5′TOP mRNAs, through the binding to 3′ terminus of the poly(A) tail.

1. Introduction

It is known that the terminal structure of RNA is important for its stability and functions. Eukaryotic mRNAs are protected from exoribonuclease activity because they are blocked at their 5′ termini with a 7-methylguanosine cap structure and 3′ poly(A) tail [1]. Eukaryotic translation initiation factor 4E (eIF4E) binds directly to the 5′ cap and facilitates translation by recruiting the ribosome to the mRNA through its interaction with eIF4G [2]. Poly(A) binding proteins (PABPs) specifically interact with the poly(A) tail and protect it from 3′ to 5′ exoribonuclease activity. The cytosolic isoforms of PABP interact with eIF4G and form characteristic loop structures, which are thought to enhance translational efficiency [2,3]. Additionally, numerous replication-dependent histone mRNAs in metazoan possess a specific stem-loop structure at their 3′ end replacing a poly(A) tail [4].

Several RNA-binding proteins specifically interact with the termini of other RNA molecules. For example, the La protein, also called La-related protein 3 (LARP3), specifically recognizes the oligo(U) terminus of nascent RNA polymerase III transcripts [5]. Similarly, LARP7 specifically recognizes the 3′ terminus of 7SK RNA and inhibits its degradation [6]. Both La protein and LARP7 belong to the La motif-related protein family, characterized by the presence of a conserved La motif [7]. Previous structural analyses of La protein have suggested a high affinity between the conserved La motif and UUU-OH at the 3′ terminus of an RNA molecule [8–10].

LARP1, one of the La-motif related proteins, was originally identified in *Drosophila* and found to be required for spermatogenesis, embryogenesis and cell cycle progression [11–13]. LARP1 is required for ordered mitosis, cell survival and cell migration in HeLa cells [14]. LARP1 also interacts with PABPs, suggesting the involvement of LARP1 in mRNA translation or its regulation [13,14]. However, there is some uncertainty regarding the specific RNA molecular targeted by LARP1.

Recently, we developed a refined method allowing comprehensive search of RNA–protein interactions using proteomics analysis of *in vitro* assembled ribonucleoproteins (RNPs) by immunoprecipitation. This method uses FLAG-conjugated *in vitro* transcribed RNA as bait in an ultrasensitive mass spectrometry system. Using this approach, we identified uncharacterized regulatory factors that bind to the 3′ untranslated region (UTR) of specific mRNA sets (unpublished data). Using this method, we also succeeded in enriching the endogenous U7 small nuclear ribonucleoprotein complex (snRNP) using a modified FLAG-tagged locked nucleic acid (LNA) antisense oligonucleotide [15].

Here, we performed a comprehensive proteomic analysis to identify proteins that recognized the 3′ terminus of the mRNA poly(A) tail, since the factors that associate with poly(A) tail, with the exception of PABP, have not been fully investigated.

* Corresponding author. Fax: +81 3 3599 8134.
E-mail address: t-natsume@aist.go.jp (T. Natsume).
[1] These authors contributed equally to this work.

0014-5793/$36.00
http://dx.doi.org/10.1016/j.febslet.2013.05.035

2. Materials and methods

2.1. Cell culture and RNA interference (RNAi)

HEK293 cells were cultured in Dulbecco's modified Eagle's medium supplemented with 10% fetal calf serum in 10-cm dishes and were grown at 37 °C in 5% CO_2. Stealth Select RNAi™ siRNAs for LARP1 (HSS118648 and HSS118649) were obtained from Life Technologies Co. (Carlsbad, CA, USA). Stealth™ RNAi Negative Control Medium GC Duplex and Medium GC Duplex #3 (Life Technologies Co.) were used as negative controls. Cells were grown in 10-cm culture dishes and were transfected with 100 pmol of short interfering RNAs (siRNAs) using Lipofectamine™ RNAiMAX (Life Technologies Co.), and were thereafter cultured at 37 °C for 48 h. The effects of RNAi were examined by qRT-PCR and Western blotting using anti-LARP1 antibody (1:1000 dilution, A302-087A, Bethyl Laboratories Inc., Montgomery, TX, USA) and anti-β-actin antibody (1:1000; #4970, Cell Signaling Technology, Danvers, MA, USA).

2.2. Preparation of in vitro transcribed RNA

To clone a portion of the partial human β-actin (ACTB) cDNA fragment containing the poly(A) sequence, a cDNA library was made using total RNA purified from HEK293 cells, and primer 2199. All of the primer sequences appear in Supplementary Table 1. The ACTB 3′ UTR sequence was amplified by polymerase chain reaction (PCR) from the cDNA library with primers 2283 and 2201, which contained the T7 promoter and complementary sequence for the LNA bait. Amplicons were cloned into pGEM-T Easy (Promega Co., Madison, WI, USA). Following sequence confirmation, the plasmid which we designated pGEM-T7_7SKtag_ACTB3U_A60, was digested with *Eco*RI and *Bsa*I, and the resulting fragment was gel-purified. Various derivative DNA templates for *in vitro* transcription were PCR amplified from pGEM-T7_7SKtag_ACTB3U_A60 using primer sets 2549, 2550, 2568, 2559, 2560, 2561, 2551, 2553, 2575, 2576, 2577, 2578, 2579, 2580, 2581 or 2201. The amplified PCR fragments were gel-purified.

In vitro transcription was carried out using a T7 mMESSAGE machine or T7 MEGAscript kit (Life Technologies Co.). Transcribed RNA was purified with MicroSpin G-25 columns (GE Healthcare Life Science, Little Chalfont, UK).

2.3. RNA-directed immunoprecipitation

A synthesized LNA177 (5′-AccuuGAGAGcuuGuuuGGAGg-3′, where uppercase represents the LNA nucleotides and lowercase represents a ribonucleotide) was obtained from Gene Design Inc. (Osaka, Japan). The LNA177 and *in vitro* transcribed RNAs were subjected to FLAG conjugation as described in Kourouklis et al. [16] with some modifications.

For annealing, 100 pmol of *in vitro* transcribed RNA and 50 pmol of FLAG-tagged LNA177 were mixed in wash buffer [20 mM Hepes·NaOH, pH 7.5, 150 mM NaCl, 0.1% Triton-X100] and denatured at 95 °C for 1 min, followed by incubation at room temperature for 5 min. The LNA/RNA complex was bound to ANTI-FLAG M2 agarose produced in mice (Sigma–Aldrich Co., St. Louis, MI, USA).

The HEK293 cells grown in 10-cm dishes were lysed with 20 mM Hepes·NaOH, pH 7.5, 150 mM NaCl, 50 mM NaF, 1 mM Na_3VO_4, 1% digitonin, 1 × complete EDTA-free protease inhibitor cocktail (Roche Applied Science, Penzberg, Upper Bavaria, Germany) The immunoprecipitation using a pre-washed RNA/LNA-FLAG/antibody complex was performed with the cell lysate. The immunoprecipitated products were eluted with 50 μg/μl FLAG peptide in wash buffer. The samples collected were analyzed by Western blotting or mass spectrometry [17].

For Western blotting, immunoprecipitated proteins were electrophoresed on a 10% sodium dodecyl sulfate (SDS) polyacrylamide gel and then blotted onto a polyvinylidene difluoride (PVDF) membrane. Antibodies used for Western blotting were as follows: LARP1 (1:1000 dilution, A302-087A, Bethyl Laboratories Inc.), PABP1 (1:1000; #4992, Cell Signaling Technology), PARN (1:1000; #3894S, Cell Signaling Technology) and eIF4G (1:1000; A301-776A, Bethyl Laboratories Inc.).

2.4. Immunoprecipitation

Immunoprecipitation of LARP1 protein was performed with the LARP1 antibody (500 ng; A302-087A or A302-088A, Bethyl Laboratories Inc.) bound to Dynabeads Protein G (Life Technologies Co.). Cell lysates were prepared as described earlier. For digestion of the poly(A) sequence, the immunoprecipitated product was incubated with 1 unit of RNase I at 37 °C for 15 min just before the second washing step.

3. Results

3.1. Comprehensive searches for interacting proteins

We prepared a modified LNA antisense oligonucleotide conjugating FLAG peptide (LNA177) and artificial mRNA-like transcript derived from a part of the human ACTB 3′ UTR sequence, which contained a 5′ cap and 3′ poly(A) tail. Briefly, components of the messenger ribonucleoprotein complexes (mRNPs) assembled on the *in vitro* transcribed mRNA annealed with FLAG-conjugating LNA177 were identified by precipitating the mRNPs with the anti-FLAG antibody. Next, the precipitated proteins were extensively characterized by highly sensitive direct nanoflow liquid chromatography/tandem mass spectrometry (LC/MS) (Fig. 1A). The detailed structures of the CAP-A60 RNA and CAP-A60 + EX RNA from the comprehensive protein analysis are shown in Fig. 1B. The CAP-A60 RNA contains a 5′ cap, a 60-nt 3′ poly(A) tail, and the complementary sequence of the antisense LNA177. The CAP-A60 + EX RNA structure contains an extra 35-nt sequence at the 3′ terminus. Mass spectrometry analyses was conducted twice for each immunoprecipitation product (Supplementary Table 2). LNA177 lacking mRNA-like bait RNA was used as a negative immunoprecipitation control.

We identified 179 proteins as the component of the mRNPs assembled with CAP-A60 RNA and CAP-A60 + EX RNA, including well-known proteins that bind to the mRNA 5′ cap or poly(A) tail (eIF4E, eIF4G and PABPs). Interestingly, several proteins such as PARN, PATL1 and LARP1 that uniquely bound to RNAs with the normal 3′ poly(A) tail (CAP-A60) were identified (Fig. 1C and Supplementary Table 2). We were particularly interested in LARP1, as some members of the LARP family are reported to recognize the 3′ termini of certain RNA molecules [5,6].

3.2. LARP1 interacts with poly(A)+ RNA

To confirm the interaction of LARP1 with poly(A)+ RNAs, we conducted further immunoprecipitation experiments with a variety of bait RNAs (Fig. 1B). LARP1 bound to A60 RNA and CAP-A60 RNA, both of which contained a genuine 3′ poly(A) terminus. LARP1 did not bind to the RNAs possessing 60-nt poly(A) stretch; nevertheless the 3′ terminus was modified by adding of sequence insertions and/or the conjugating FLAG peptide (Fig. 1C). It is noteworthy that PABP1 interacted with all of the mRNAs containing a poly(A) stretches that were examined, regardless of their 3′ terminal structure (Fig. 1C). Additionally, the presence of a 5′ cap did not affect LARP1 binding to the poly(A)+ RNA (Fig. 1C).

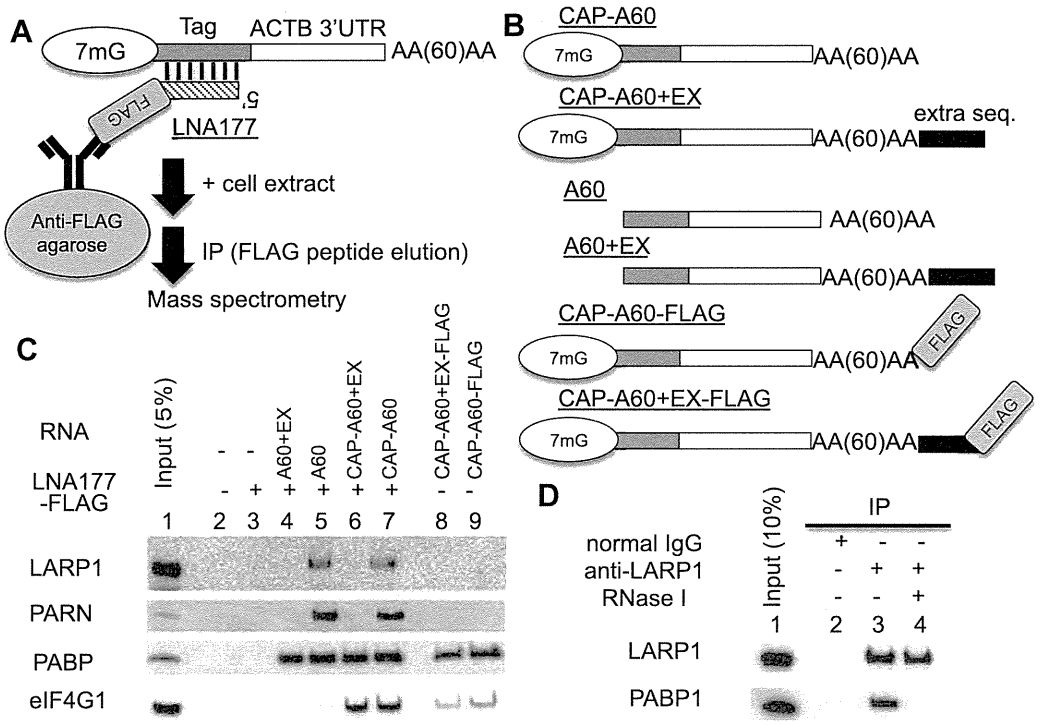

Fig. 1. Identification of proteins assembled on artificial poly(A)+ mRNA by LNA/RNA immunoprecipitation following ultra sensitive mass spectrometry. (A) Purification strategy for RNA immunoprecipitation using FLAG-tagged antisense LNA177. FLAG-tagged LNA177 and bait mRNA were annealed and then bound to anti-FLAG M2 agarose. The complex was then incubated with a HEK293 cell lysate. After washing, immunoprecipitated proteins were digested with lysyl endopeptidase and analyzed by LC–MS. (B) Schematic of the *in vitro* transcribed bait RNA used in the RNA immunoprecipitation assays. All chimeric mRNA shared the 3′ UTR of ACTB mRNA, a complementary sequence to LNA177, and a 60-nt poly(A) tail. The 35-nt of extra sequence (5′-GAGACCACUGUCAUGCCGUUACGUAGAAUCGAAUU) was derived from pGEM T-Easy vector (Promega) and primer 2199 using cDNA cloning for the ACTB 3′UTR possessing poly(A) tail. (C) Co-immunoprecipitated proteins with various bait RNAs were analyzed by Western blotting. Lane 1, input; 2, no bait; 3, LNA177; 4, LNA177 + A60 + EX RNA; 5, LNA177 + A60 RNA; 6, LNA177 + CAP-A60 + EX RNA; 7, LNA177 + CAP-A60 RNA; 8, LNA177 + CAP-A60 + EX-FLAG RNA and 9, LNA177 + CAP-A60-FLAG RNA. (D) RNA dependent interaction of LARP1 and PABP1. Immunoprecipitation of LARP1 was performed with an anti-LARP1 antibody (A302-088A, Bethyl Laboratories Inc.). IgG was used as a control. Part of the immunoprecipitated sample was treated with RNase I to digest the poly(A) sequences. The immunoprecipitated proteins were analyzed by Western blotting using antibodies against LARP1 and PABP1. Lane 1, input; 2, normal IgG; 3, anti-LARP1; and 4, anti-LARP1 + RNase I treatment.

Next, we confirmed the intracellular interaction of LARP1 with PABP1 by immunoprecipitation using an anti-LARP1 antibody. The LARP1–PABP1 interaction of was disintegrated by RNase I treatment, suggesting that the interaction was RNA dependent (Fig. 1D).

3.3. Sequence specificity of LARP1 RNA recognition

To assess the length of poly(A) tail required for LARP1 binding, we carried out further RNA immunoprecipitation with RNA possessing poly(A) tail of various lengths. It was apparent that LARP1 binding required a poly(A) tail longer than 9-nt (Fig. 2A and B). To determine the nucleotide selectivity of LARP1, we prepared various RNA baits with different nucleotide compositions and analyzed their interaction with LARP1 by RNA immunoprecipitation. LARP1 did not bind to mutant RNAs possessing poly(G), poly(C) or poly(U) sequences at their 3′ termini (Fig. 2C and D). Furthermore, the LARP1 with poly(A)+ RNA interaction was abolished by adding a single guanosine, cytidine or uridine residue to the 3′ terminus of the RNA (Fig. 2C and D).

3.4. LARP1 stabilizes multiple 5′TOP mRNAs

To confirm the specific interaction of LARP1 with poly(A)+ mRNA under physiological conditions, we immunoprecipitated endogenous LARP1 protein using two different LARP1 antibodies (Fig. 3A). Co-immunoprecipitated RNAs were purified and analyzed by qRT-PCR. We confirmed that all of the mRNAs possessing a 3′ poly(A) tail that were examined were enriched in the anti-LARP1 immunoprecipitations (Fig. 3B). In contrast, no enrichment of RNA species lacking poly(A) tail, such as ribosomal RNAs, nuclear non-coding RNAs (ncRNAs) and histone mRNAs, were detected.

We hypothesized that LARP1 was involved in stabilization of poly(A)+ mRNAs through binding to the 3′ terminus of the poly(A) tail. To confirm this, we conducted LARP1 depletion using RNAi in HEK293 cells (Fig. 4A and B). Then we investigated the accumulation levels of numerous transcripts, which were commonly used for reference (Fig. 4C, E and F).

Unexpectedly, PP1A, YWHAZ, PGK1, TBP1, GAPDH, HSP90AB1, TBX1 and PRCP mRNAs were slightly altered by depletion of LARP1, although these mRNAs were co-immunoprecipitated with the anti-LARP1 antibody (Figs. 3B and 4E). We also confirmed that the levels of several ncRNAs and histone mRNAs, which were not co-immunoprecipitated with anti-LARP1 antibody, were unaltered (Figs. 3B and 4F). Interestingly, the levels of mature mRNAs for RPS6, RPL7 and HNRNPA1 were substantially diminished, while the levels of the corresponding unspliced pre-mRNAs remained constant in the LARP1-depleted cells (Fig. 4C).

RPS6, RPL7 and HNRNPA1 mRNAs were categorized as 5′TOP mRNAs [18,19]. Therefore, we examined the expression levels of other eight 5′TOP RNAs, and found that the expression levels of those examined were commonly reduced by LARP1 depletion (Fig. 4D).

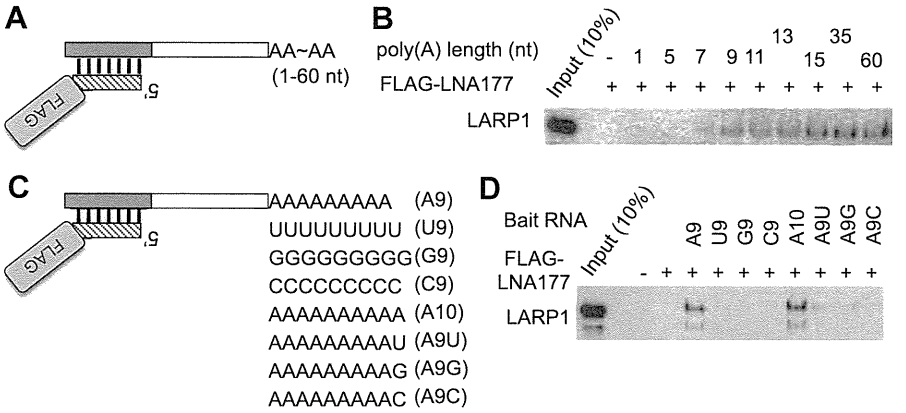

Fig. 2. LARP1 specifically recognized the 3′ terminus of a poly(A) tail. (A) Schematic of bait RNAs with poly(A) tails of various lengths. (B) The binding specificity of LARP1 to poly(A) tails of various lengths was examined by RNA immunoprecipitation and the products were analyzed by Western blotting using an antibody against LARP1. (C) Schematic of mutant mRNAs with a variety of 3′ termini. An A9 RNA with a 9-nt poly(A) tail was used as a positive standard. The 3′ terminus of three variants (U9, G9, and C9; upper panel) was consist of 9 nt for poly(G), poly(C) or poly(U), instead of poly(A). The four variants (10A, A9G, A9C and A9U; lower panel) contained an extra nucleotide at the 3′ end of the poly(A) tail. (D) RNA immunoprecipitation and Western blot analysis as shown in (B).

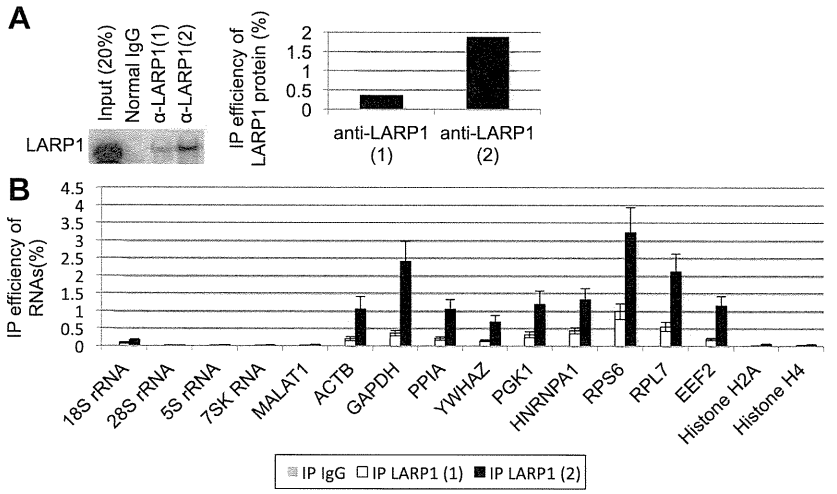

Fig. 3. LARP1 commonly interacts with poly(A)+ RNA. (A) Immunoprecipitation with normal IgG as a control and two different antibodies against LARP1 (1; A302-087A or 2; A302-088A, Bethyl Laboratories Inc.) were conducted. The representative immunoprecipitated LARP1 proteins were evaluated by Western blotting (left) and the immunoprecipitation efficiency of LARP1 was quantified by Multi Gauge ver. 3.0 software (Fujifilm, Japan. right). (B) RNAs that co-immunoprecipitated with LARP1 were purified for qRT-PCR analysis. Multiple sets of primers for ribosomal RNAs, nuclear ncRNAs, mRNAs encoding reference genes, and histone mRNAs, were prepared as shown in Supplementary Table 1. Bars represent means ± S.D. of three independent experiments.

4. Discussion

In this study, we attempted to identify the proteins that bind to the poly(A) termini of mRNA molecules by RNA-immunoprecipitation and following ultra-sensitive mass spectrometry. A comparison of proteins that interact with CAP-A60 RNA and CAP-A60 + EX RNA revealed several candidate proteins, which specifically interacted with the 3′ terminus of a poly(A) tail (Supplementary Table 2).

Among these candidate proteins, we observed that LARP1 specifically recognized the 3′ termini of poly(A) tails (Fig. 1C). We also showed that a length >9-nt in the 3′ terminal poly(A) tail was necessary for the LARP1 binding (Fig. 2B). Additionally, a slight increase in the LARP1 signal was observed when the poly(A) tail length was increased from 13-nt to 15-nt. However, further elongation of the tail did not affect LARP1 binding (Fig 2B). Hence, we consider that a poly(A) of at least 9-nt is the minimum for the RNA recognition by LARP1, while 15-nt poly(A) is sufficient.

Previous studies have shown that the conserved La motif of La protein specifically recognizes the 3′ terminal UUU sequence on the nascent transcripts of RNA polymerase III [5]. It is noteworthy that the 3′-hydroxyl group and a penultimate base mainly affected to the La protein affinity for RNA, while the last nucleotide appeared to be less important [8–10]. It should be noted that addition of an extra G, C or U at the 3′ terminus of the poly(A) tail diminished LARP1 recruitment onto the synthetic RNA (Fig. 2D), regardless of its possession of the highly conserved La motif [9]. Further analyses are required to clarify the mechanism by which the poly(A) terminal binds to LARP1.

We showed that the poly(A)+ mRNA interaction preference exhibited by LARP1 differed from those exhibited by PABP1 (Fig. 1C). These results imply that LARP1 is recruited onto the 3′ terminus of poly(A) tail, independently with of PABP1. However, a previous study reported that LARP1 directly interacted with PABP, as shown RNase A treatment, which cleaves specifically after pyrimidine nucleotides [15]. Because both LARP1 and PABP

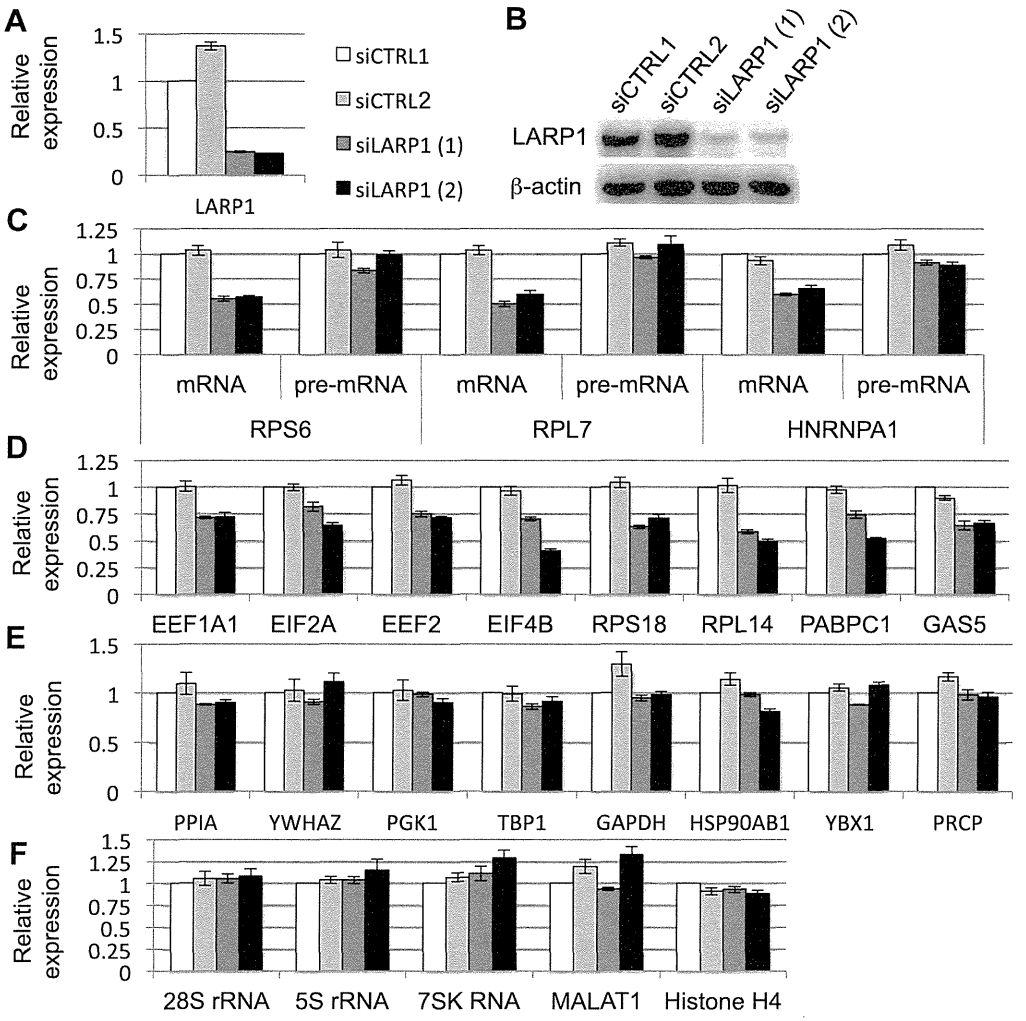

Fig. 4. LARP1 stabilized 5′TOP mRNAs. RNAi using negative control siRNAs (open and light gray bars) and two different siRNAs for LARP1 (dark gray and black bars) were conducted in HEK 293 cells. RNAi showing diminished levels of LARP1 mRNA (A) and protein (B). The expression levels of multiple RNAs were examined by qRT-PCR. Relative expression levels of the RNAs examined were normalized against 18S rRNA. Bars represent the means ± S.D. of three independent experiments. (C) Matured and immatured 5′ TOP mRNAs, (D) other 5′TOP RNAs, (E) reference mRNAs, and (F) non-coding RNAs and histone mRNA.

interacted with poly(A), our interaction analysis was performed by RNase I treatment, and revealed the RNA dependent interaction of LARP1 with PABP1 at least in human cells (Fig. 1D).

Meanwhile, in drosophila, it was reported that the interaction with dmLarp and pabp have been reported to resistant to RNase I digestion [13]. It is possible that a low conservation rate in the N-terminal region of LARP1 was the cause of the distinct affinity to PABP observed in our study.

The poly(A) tail plays a critical role in translational activation and stabilization of mRNA [1], whereas a previous study showed that LARP1 promotes the translation [14]. Our results showed that a large portion of mRNAs possessing poly(A) tail were co-immunoprecipitated with LARP1 (Fig. 3) and LARP1 depletion caused a decrease in the expression levels of 5′TOP mRNA (Fig. 4C and D). We asked whether the reduction of these mRNAs was regulated transcriptionally or post-transcriptionally. Accordingly, expression of RPS6, RPL7, and HNRNPA1 pre-mRNA was constant, thus that the reduction in mRNA was post-transcriptional event, and one of which was perhaps related to RNA stability.

We assumed that LARP1 might contribute to the mRNA stabilization by preventing the 3′–5′ exoribonuclease activity. To investigate whether the reduction of 5′TOP mRNA was due to shortening of the poly(A) tail, we conducted northern blot analysis of RPS6 and RPL7 mRNAs. However, no obvious shortening of these mRNAs was detected in the LARP1-depleted cells (data not shown).

It remains unclear as to why LARP1 depletion only affects 5′TOP mRNA, although LARP1 commonly interacted with poly(A)+ mRNA (Fig. 3B). The 5′TOP mRNAs tend to be the most abundant poly(A)-containing mRNAs in the cell. To examine the effects of RNA abundance, we examined GAPDH, HSP90AB1, YBX1 and PRCP mRNAs, which showed similar abundances to 5′TOP mRNAs in HEK293 cells; slight alternation of these mRNAs was revealed by RNAi for LARP1 (Fig. 4E).

A previous study showed that the LARP1 orthologous in *Caenorhabditis elegans* localizes to the P-body [20], where translationally inactivated mRNAs accumulate and are usually subjected to degradation [21,22]. It is consistent that LARP1 affects the stability of the translationally inactivated mRNA including majority of 5′TOP RNAs.

Previous reports have indicated that La protein has affinity for the 5′ cap and 5′ triphosphate of RNA molecules, and LARP7 interacted with 5′ end of RNA with methylphosphate capping enzyme dependent manner [23–25]. It is also reasonable to speculate that LARP1 may control mRNA stability by mediating the interaction

between 5′TOP at the 5′ terminus and poly(A) tail at the 3′ terminus of an mRNA.

In this study, we showed that the LARP1 recognized the 3′ terminus of an mRNA poly(A) tail and selectively stabilized 5′TOP mRNAs. The biological function and true significances of the LARP1–mRNA interaction at the 3′ terminus of the a poly(A) tail remains unclear. Investigation in the mechanisms involved in LARP1-mediated stabilization of 5′TOP mRNA and into the physiological role(s) of LARP1 are planned.

Acknowledgements

We thank the members of the Natsume laboratory for their valuable discussion and assistance. We also thank Dr. Tetsuro Hirose for providing useful advices and comments on the manuscript. This research was supported by a Grant from the New Energy and Industrial Technology Development Organization (NEDO).

Appendix A. Supplementary data

Supplementary data associated with this article can be found, in the online version, at http://dx.doi.org/10.1016/j.febslet.2013.05.035.

References

[1] Parker, R. and Song, H. (2004) The enzymes and control of eukaryotic mRNA turnover. Nat. Struct. Mol. Biol. 11, 121–127. Review.
[2] Jackson, R.J., Hellen, C.U. and Pestova, T.V. (2010) The mechanism of eukaryotic translation initiation and principles of its regulation. Nat. Rev. Mol. Cell Biol. 11, 113–127. Review.
[3] Mangus, D.A., Evans, M.C. and Jacobson, A. (2003) Poly(A)-binding proteins: multifunctional scaffolds for the post-transcriptional control of gene expression. Genome Biol. 4, 223. Review.
[4] Dominski, Z. and Marzluff, W.F. (2007) Formation of the 3′ end of histone mRNA: getting closer to the end. Gene 396, 373–390.
[5] Stefano, J.E. (1984) Purified lupus antigen La recognizes an oligouridylate stretch common to the 3′ termini of RNA polymerase III transcripts. Cell 36, 145–154.
[6] Krueger, B.J., Jeronimo, C., Roy, B.B., Bouchard, A., Barrandon, C., Byers, S.A., Searcey, C.E., Cooper, J.J., Bensaude, O., Cohen, E.A., Coulombe, B. and Price, D.H. (2008) LARP7 is a stable component of the 7SK snRNP while P-TEFb, HEXIM1 and hnRNP A1 are reversibly associated. Nucleic Acids Res. 36, 2219–2229.
[7] Bousquet-Antonelli, C. and Deragon, J.M. (2009) A comprehensive analysis of the La-motif protein superfamily. RNA 15, 750–764.
[8] Teplova, M., Yuan, Y.R., Phan, A.T., Malinina, L., Teplov, A. and Patel, D.J. (2006) Structural basis for recognition and sequestration of UUU(OH) 3′ temini of nascent RNA polymerase III transcripts by La, a rheumatic disease autoantigen. Mol. Cell 21, 75–85.
[9] Dong, G., Chakshusmathi, G., Wolin, S.L. and Reinisch, K.M. (2004) Structure of the La motif: a winged helix domain mediates RNA binding via a conserved aromatic patch. EMBO J. 23, 1000–1007.
[10] Bayfield, M.A., Yang, R. and Maraia, R.J. (2010) Conserved and divergent features of the structure and function of La and La-related proteins (LARPs). Biochim. Biophys. Acta 1799, 365–378.
[11] Ichihara, K., Shimizu, H., Taguchi, O., Yamaguchi, M. and Inoue, Y.H. (2007) A Drosophila orthologue of larp protein family is required for multiple processes in male meiosis. Cell Struct. Funct. 32, 89–100.
[12] Chauvet, S., Maurel-Zaffran, C., Miassod, R., Jullien, N., Pradel, J. and Aragnol, D. (2000) Dlarp, a new candidate Hox target in Drosophila whose orthologue in mouse is expressed at sites of epithelium/mesenchymal interactions. Dev. Dyn. 218, 401–413.
[13] Blagden, S.P., Gatt, M.K., Archambault, V., Lada, K., Ichihara, K., Lilley, K.S., Inoue, Y.H. and Glover, D.M. (2009) Drosophila Larp associates with poly(A)-binding protein and is required for male fertility and syncytial embryo development. Dev. Biol. 334, 186–197.
[14] Burrows, C., Abd Latip, N., Lam, S.J., Carpenter, L., Sawicka, K., Tzolovsky, G., Gabra, H., Bushell, M., Glover, D.M., Willis, A.E. and Blagden, S.P. (2010) The RNA binding protein Larp1 regulates cell division, apoptosis and cell migration. Nucleic Acids Res. 38, 5542–5553.
[15] Ideue, T., Adachi, S., Naganuma, T., Tanigawa, A., Natsume, T. and Hirose, T. (2012) U7 small nuclear ribonucleoprotein represses histone gene transcription in cell cycle-arrested cells. Proc. Natl. Acad. Sci. USA 109, 5693–5698.
[16] Kourouklis, D., Murakami, H. and Suga, H. (2005) Programmable ribozymes for mischarging tRNA with non-natural amino acids and their applications to translation. Methods 36, 239–244.
[17] Natsume, T., Yamauchi, Y., Nakayama, H., Shinkawa, T., Yanagida, M., Takahashi, N. and Isobe, T. (2002) A direct nanoflow liquid chromatography–tandem mass spectrometry system for interaction proteomics. Anal. Chem. 74, 4725–4733.
[18] Meyuhas, O. (2000) Synthesis of the translational apparatus is regulated at the translational level. Eur. J. Biochem. 267, 6321–6330. Review.
[19] Thoreen, C.C., Chantranupong, L., Keys, H.R., Wang, T., Gray, N.S. and Sabatini, D.M. (2012) A unifying model for mTORC1-mediated regulation of mRNA translation. Nature 485, 109–113.
[20] Nykamp, K., Lee, M.H. and Kimble, J. (2008) *C. elegans* La-related protein, LARP-1, localizes to germline P bodies and attenuates Ras-MAPK signaling during oogenesis. RNA 14, 1378–1389.
[21] Parker, R. and Sheth, U. (2007) P bodies and the control of mRNA translation and degradation. Mol. Cell 25, 635–646.
[22] Moser, J.J. and Fritzler, M.J. (2010) Cytoplasmic ribonucleoprotein (RNP) bodies and their relationship to GW/P bodies. Int. J. Biochem. Cell Biol. 42, 828–843.
[23] Fan, F., Goodier, J.L., Chamberlain, J.R., Engelke, D.R. and Maraia, R.J. (1998) 5′ Processing of tRNA precursors can be modulated by the human La antigen phosphoprotein. Mol. Cell. Biol. 18, 3201–3211.
[24] Bhattachary, R., Perumal, K., Sinha, K., Maraia, R. and Reddy, R. (2002) Methylphosphate cap structure in small RNAs reduces the affinity of RNAs to La protein. Gene Expr. 10, 243–253.
[25] Muniz, L., Egloff, S. and Kiss, T. (2013) RNA elements directing in vivo assembly of the 7SK/MePCE/Larp7 transcriptional regulatory snRNP. Nucleic Acids Res. 41, 4686–4698.

jmb Article

PLEIAD/SIMC1/C5orf25, a Novel Autolysis Regulator for a Skeletal-Muscle-Specific Calpain, CAPN3, Scaffolds a CAPN3 Substrate, CTBP1

Yasuko Ono[1,2], Shun-ichiro Iemura[1,3], Stefanie M. Novak[2], Naoko Doi[1], Fujiko Kitamura[1], Tohru Natsume[3], Carol C. Gregorio[2] and Hiroyuki Sorimachi[1]

*1 - **Calpain Project,** Department of Advanced Science for Biomolecules, Tokyo Metropolitan Institute of Medical Science (IGAKUKEN), 2-1-6 Kamikitazawa, Setagaya-ku, Tokyo 156-8506, Japan*
*2 - **Cellular and Molecular Medicine,** University of Arizona, Tucson, AZ 85724, USA*
*3 - **Biological Information Research Center,** National Institute of Advanced Industrial Science and Technology, 2-42 Aomi, Kohtoh-ku, Tokyo 135-0064, Japan*

***Correspondence to Yasuko Ono:** Calpain Project, Department of Advanced Science for Biomolecules, Tokyo Metropolitan Institute of Medical Science, 2-1-6 Kamikitazawa, Setagaya-ku, Tokyo 156-8506, Japan. ono-ys@igakuken.or.jp*
http://dx.doi.org/10.1016/j.jmb.2013.05.009
Edited by R. Huber

Abstract

CAPN3/p94/calpain-3 is a skeletal-muscle-specific member of the calpain protease family. Multiple muscle cell functions have been reported for CAPN3, and mutations in this protease cause limb-girdle muscular dystrophy type 2A. Little is known about the molecular mechanisms that allow CAPN3 to be so multifunctional. One hypothesis is that the very rapid and exhaustive autolytic activity of CAPN3 needs to be suppressed by dynamic molecular interactions for specific periods of time. The previously identified interaction between CAPN3 and connectin/titin, a giant molecule in muscle sarcomeres, supports this assumption; however, the regulatory mechanisms of non-sarcomere-associated CAPN3 are unknown. Here, we report that a novel CAPN3-binding protein, PLEIAD [*Pl*atform *e*lement for *i*nhibition of *a*utolytic *d*egradation; originally called SIMC1/C5orf25 (*S*UMO-*i*nteracting *m*otif *c*ontaining protein *1*/*c*hromosome *5* *o*pen *r*eading *f*rame *25*)], suppresses the protease activity of CAPN3. Database analyses showed that PLEIAD homologs, like CAPN3 homologs, are evolutionarily conserved in vertebrates. Furthermore, we found that PLEIAD also interacts with CTBP1 (*C*-*t*erminal *b*inding *p*rotein *1*), a transcriptional co-regulator, and CTBP1 is proteolyzed in COS7 cells expressing CAPN3. The identified cleavage sites in CTBP1 suggested that it undergoes functional modification upon its proteolysis by CAPN3, as well as by conventional calpains. These results indicate that PLEIAD can shift its major function from CAPN3 suppression to CAPN3-substrate recruitment, depending on the cellular context. Taken together, our data suggest that PLEIAD is a novel regulatory scaffold for CAPN3, as reflected in its name.

Introduction

CAPN3 (also called p94 or calpain-3) is an skm (*sk*eletal *m*uscle)-specific cysteine protease belonging to the calpain super family (EC 3.4.22.18, clan CA, family C2).[1] The calpains are intracellular Ca^{2+}-requiring cysteine proteases. Many studies have shown that proteolysis by calpain has a modulatory effect on the functions of the substrate proteins.[2–6] Therefore, calpain is considered to be a modulator protease rather than a degrading protease such as proteasomal and lysosomal proteases.[7]

From a physiological perspective, genetic defects in CAPN3 cause limb-girdle muscular dystrophy type 2A[8]; therefore, the importance of CAPN3's functions are well recognized.[9] To examine the consequences of altering the modulating functions of CAPN3 in skm, we have generated several different mouse limb-girdle muscular dystrophy type 2A models, including knockout mice (*Capn3*$^{-/-}$), which lack the full-length CAPN3 protein[10–17]; knockin mice (*Capn3*$^{CS/CS}$) in

which CAPN3 is replaced by a protease-inactive mutant CAPN3:C129S (CAPN3:CS)[18,19]; and transgenic mice in which CAPN3:CS is overexpressed.[20] Analyses of these models have shown that CAPN3 has different cellular functions depending on the subcellular compartment in which it is located. In particular, a surprising finding was that CAPN3 localizes to triads, where it plays an important role as a structural component and not as a protease.[19]

The two defined roles of CAPN3, that is, as a protease and as a structural protein, are not necessarily mutually exclusive. However, too little is currently known about the molecular properties of CAPN3 to explain the relationships among these two roles and another property of CAPN3—its very rapid autolysis.[21] In skm cells, CAPN3's stability as a pre-autolytic full-length molecule has been attributed to its interaction with connectin/titin, a giant sarcomeric protein,[22,23] since connectin/titin's ability to suppress the autolytic loss of CAPN3 has been shown biochemically.[24] Furthermore, the N2A region of connectin/titin has been suggested to function as a scaffold for CAPN3.[25,26] However, in skm cells, CAPN3 is stable not only in sarcomeres but also in the cytosol.[27] Therefore, it is predicted that there are other regulatory mechanisms working in parallel or in combination with the connectin/titin-based machinery, to support CAPN3's multiple functions, especially those occurring outside of sarcomeres.

We sought to identify CAPN3-interacting proteins using a highly sensitive and efficient method based on mass spectrometry for analyzing protein–protein interactions.[28] Among these proteins, PLEIAD (*Pl*atform *e*lement for *i*nhibition of *a*utolytic *d*egradation), which was the previously uncharacterized SIMC1/C5orf25 (*S*UMO-*i*nteracting *m*otif *c*ontaining protein *1*/*c*hromosome *5* *o*pen *r*eading *f*rame *25*),[29] demonstrated a suppressive effect on CAPN3's protease activity. We identified vertebrate orthologs of PLEIAD according to their similarity with the human C-terminal sequence, which harbors the CAPN3 inhibitory or regulatory activity. We also found that PLEIAD binds to CTBP1 (*C-t*erminal *b*inding *p*rotein *1*),[30,31] which is a good substrate for calpains, including CAPN3. These results suggest that SIMC1/C5orf25 is a suppressor for CAPN3 but, at the same time, scaffolds CAPN3 to direct and regulate its substrate-proteolyzing activity. Such properties, like those of the connectin/titin N2A region, would qualify PLEIAD as an important regulatory protein for CAPN3.

Results

Protease activity of CAPN3 is suppressed by a novel protein, PLEIAD

To explore molecular interactions relevant to CAPN3's function and regulation, we expressed FLAG-CAPN3:N358D (CAPN3:ND), an activity-attenuated mutant[32] (Fig. 1a), in HEK293 cells and analyzed anti-FLAG coimmunoprecipitates of HEK293 lysates by liquid chromatography coupled with tandem mass spectrometry.[28] Since the initial goal was to identify activation-dependent interactions, the cells were treated with the Ca^{2+}-ionophore A23187, and the results were compared to those obtained in cells without A23187 treatment. This approach identified a novel CAPN3-binding protein C5orf25, which we named PLEIAD (see below) (Fig. 1b). To confirm the interaction, we expressed both proteins in COS7 cells; the interaction between MYC-PLEIAD and FLAG-CAPN3, as well as the interaction between FLAG-PLEIAD and CAPN3,

Fig. 1. A novel human protein, PLEIAD/C5orf25, interacts with and suppresses CAPN3. (a) Structure of CAPN3 is schematically shown. Autolytic activity is based on the result when each construct is expressed in COS7 cells. Vertical arrows indicate predominant autolytic sites. PC1 and PC2, protease core domains 1 and 2; C2L, C2-domain-like; PEF (L), penta-EF-hand; NS/IS1/IS2, CAPN3-specific insertion sequences; C129/H334/N358, active-site amino acid residues Cys, His, and Asn; CAPN3:CS, protease-inactive mutant; CAPN3:ND, a mutant with attenuated protease activity. (b) Domain structure of hPLEIAD and its genomic structure. Transcript variants are also depicted. The sequence information is summarized in Table 2. hPLEIADa to e, known splicing variants. hPLEIADf, the novel splicing variant of PLEIAD identified in this study, which lacks exons 2 and 3. "S1" to "S3" and "AS1" to "AS4" represent the positions of sense and antisense primers, respectively, used in the study. The sequences are summarized in Table 1. Ser and Pro, Ser-rich and Pro-rich region, respectively; PEST, a region rich in Pro, Glu, Ser, and Thr; NLS, putative nuclear localization signal sequence. Two phosphorylation sites are identified in hPLEIAD, S651 and S791. (c) hPLEIADf was coexpressed with CAPN3:WT(WT) or CAPN3:CS(CS) in COS7 cells and immunoprecipitated by anti-FLAG (FLAG-IP). Both CAPN3:WT and CAPN3:CS were coimmunoprecipitated with hPLEIADf. Note that the full-length 94-kDa band was hardly detectable when CAPN3:WT was expressed alone (lane 1, anti-pIS2). In the presence of coexpressed hPLEIADf, the 94-kDa band became visible and appeared to be coimmunoprecipitated more efficiently than the 55-kDa autolyzed fragment (lanes 4 and 9). (d) When coexpressed with PLEIADa or hPLEIADf in COS7 cells, the intensity of the full-length 94-kDa band of CAPN3:WT relative to that of the 55-kDa autolyzed fragment increased (lanes 4 and 5, anti-CAPN3). In the same samples, generation of the proteolyzed fragment of fodrin was suppressed (lanes 4 and 5, anti-proteolyzed fodrin). When the amount of the expression plasmid for hPLEIADf was reduced, the effects were smaller, and a decrease in expressed hPLEIADf was observed (lane 6). Closed and open arrowheads indicate the full-length and autolytic fragments of CAPN3, respectively, detected by Western blotting using an anti-pIS2 antibody. (e) Signal intensity of the full-length 94-kDa band evaluated using the intensity of the autolytic 55-kDa band in the same lane as a standard (e).

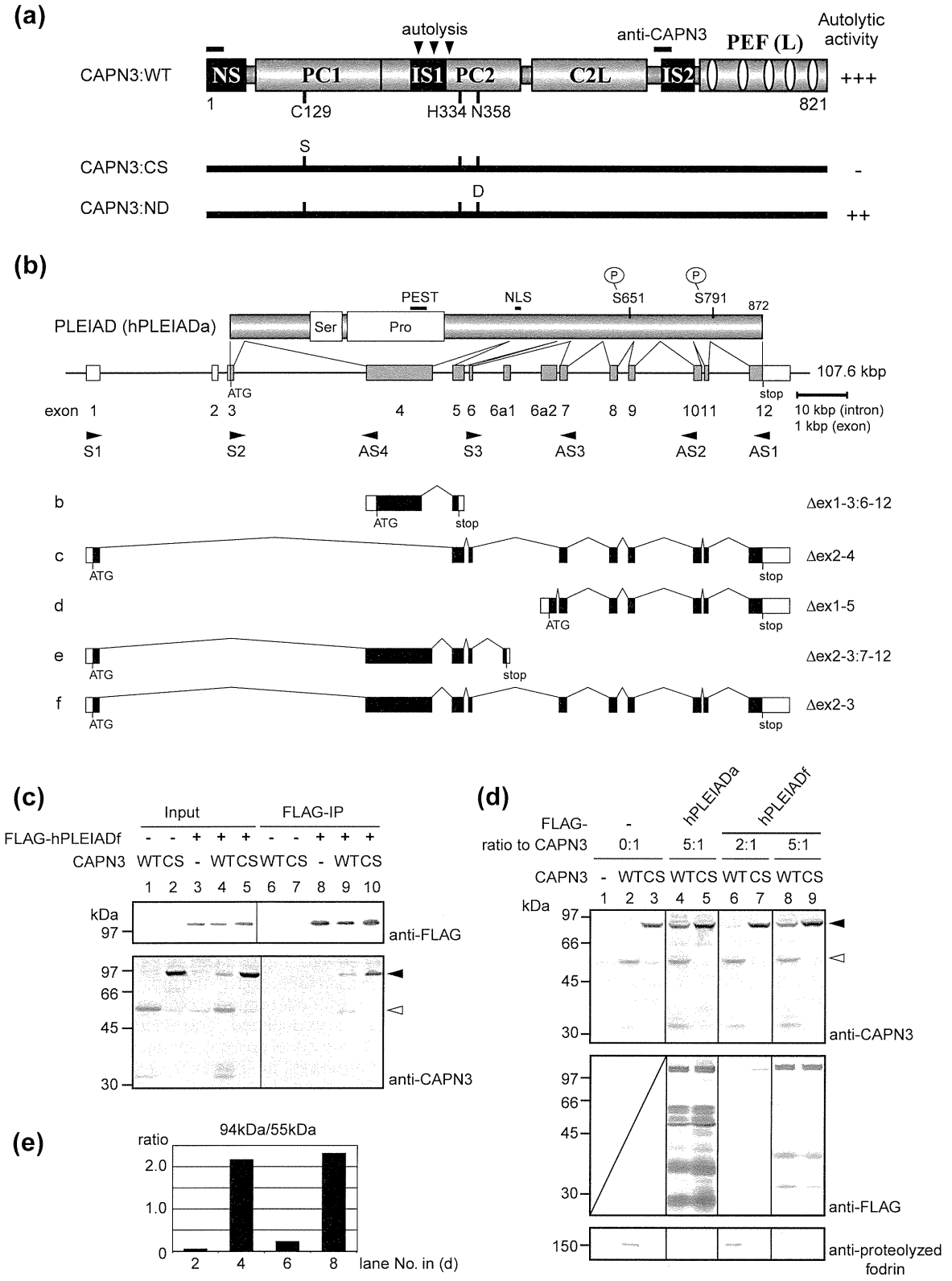

Fig. 1 (*legend on previous page*)

was reproducible without A23187 treatment (data not shown). Therefore, A23187 was omitted in the subsequent experiments.

The human PLEIAD gene (*PLEIAD*) is composed of 12 exons, of which exon 3 encodes the canonical first Met (Fig. 1b). In the National Center for Biotechnology Information (NCBI) and UniProtKB databases, the sequences for several alternative transcripts and corresponding proteins are deposited.[33] None of them, however, contains the sequence corresponding to exons 2 and 3. By PCR using a human skm cDNA library, we identified a novel variant lacking exons 2 and 3, but none of the other variants was found in the database [Fig. 1b, (5)]. This isoform will be temporarily designated as hPLEIADf.

Anti-FLAG coimmunoprecipitation experiments demonstrated the interaction of FLAG-hPLEIADf with CAPN3:WT and CAPN3:CS (Fig. 1c, lanes 9 and 10, anti-CAPN3). Therefore, the interaction between PLEIAD and CAPN3, which was originally detected in HEK293 cells, is predicted to take place in skm cells. Notably, the amount of FLAG-hPLEIADf was decreased when coexpressed with CAPN3:WT (compare lanes 4 and 5, anti-FLAG), and the relative intensity of the full-length 94-kDa band of CAPN3:WT was increased in the same sample (compare lanes 1 and 4, anti-CAPN3). This phenomenon is likely to indicate that CAPN3 activity reduces the amount of PLEIAD, either directly by proteolyzing it or indirectly by reducing the efficiency of PLEIAD's expression, and that PLEIAD reduces the autolytic activity of CAPN3.

These trends were confirmed by several independent transfections, and one representative result is shown in Fig. 1d. The signal intensity of the full-length 94-kDa band was evaluated using the intensity of the autolytic 55-kDa band in the same lane as a standard (Fig. 1e). Both hPLEIADa and hPLEIADf increased the amount of the 94-kDa CAPN3:WT, which was dependent on the level of hPLEIADf (lanes 4, 6, and 8, anti-CAPN3). Since the CAPN3-dependent proteolysis of fodrin was also suppressed (lanes 4 and 8 compared with lane 2, anti-proteolyzed fodrin), it was concluded that the protease activity of CAPN3 is suppressed by PLEIAD. Multiple bands were observed for hPLEIADa and hPLEIADf (Fig. 1d, lanes 4, 5, 8, and 9), independent of CAPN3's protease activity. Since FLAG tags were introduced to the N-termini of the hPLEIADs, the observed molecular sizes of these bands suggested that the region encoded by exon 4 is susceptible to nonspecific proteolysis in the cell.

The C-terminal region of PLEIAD regulates CAPN3's autolysis

To define the functional domains of PLEIAD with respect to their effect on CAPN3 autolysis, we coexpressed two different PLEIAD regions with CAPN3 in COS7 cells.

When the C-terminal region, designated as hPLEIAD-C, was coexpressed with CAPN3, the amount of CAPN3 detected by anti-CAPN3 increased. That is, the relative intensity of the 94-kDa band of CAPN3:WT increased, indicating reduced autolytic activity, but not as much as with the coexpression of hPLEIADa or hPLEIADf (Fig. 2b, lane 3 *versus* Fig. 1d, lanes 4 and 8, anti-CAPN3). In contrast, the N-terminal region of hPLEIAD, called hPLEIAD-N, had no effect on the expression pattern or intensity of CAPN3 (lane 4). These findings suggested that the conserved C-terminal sequence retained the CAPN3-suppressing activity, although it was weaker than the suppression exerted by full-length hPLEIADa and hPLEIADf.

For the mouse PLEIAD ortholog (mPLEIAD, originally called LOC319719), the structure of its gene, *Pleiad* (originally called *4732471D19Rik*), is similar to that of human *PLEIAD* (Fig. 2c). There are,

Fig. 2. The C-terminal region of PLEIAD is responsible for regulating CAPN3's autolytic activity. (a) Two regions of PLEIAD, hPLEIAD-N [corresponding to exons 1–4, lacking the sequence from 368 aa to 458 aa (91 aa) and having an additional sequence, LDICCSP, in its C-terminus] and hPLEIAD-C (exons 5–12) were coexpressed with CAPN3:WT or CAPN3:CS in COS7 cells. PLEIAD homologs identified by psi-BLAST search share homology with the sequence of hPLEIAD-C (Tables 2 and 3). (b) When the C-terminal region, hPLEIAD-C, was coexpressed, the 94-kDa band of CAPN3:WT was visible (lane 3). However, the effect was not as dramatic as that observed with full-length PLEIAD (Fig. 1d, lanes 4 and 8). Notably, in the same sample, the intensity of the bands for autolyzed fragments was increased. The same patterns were observed for cells in which CAPN3:CS was coexpressed with either fragment of PLEIAD (lanes 6 and 7). Closed and open arrowheads indicate the full-length and autolytic fragments of CAPN3, respectively, detected by Western blotting using an anti-pIS2 antibody. (c) Mouse PLEIAD, mPLEIAD/LOC319719, is encoded by *Pleiad* (originally called *4732471D19Rik*). In this gene, the exons corresponding to exons 2 and 3 in the human *PLEIAD* are not defined. The largest gene product (mPLEIADa) is composed of 1354 aa, which is much larger than any isoforms of hPLEIAD. The structure of mPLEIADb is essentially identical with that of hPLEIADc. S3 and AS2 indicate the position of primers used in (d). The primer sequences are summarized in Table 1. (d) Expression of *Pleiad* detected by RT-PCR. In myotubes, a splicing variant of CAPN3 without exons 15 and 16 was also faintly detected (lane 11, lower band). W, H_2O was used as a template; – and +, isolated total RNA before and after, respectively, the RT reaction, was used as template; M, size marker. Qc, quadriceps from a 30-week-old mouse; Mt5, myotubes developed for 5 days from a primary culture of mouse myoblasts. Expected product sizes for *Capn3* (by primers CAPN3_411 and 412) and *Pleiad* (S3 and AS2) were 547 bp and 492 bp, respectively.